

# Effect of metamorphic reactions on thermal evolution in collisional orogens

T. LYUBETSKAYA AND J. J. AGUE

Department of Geology and Geophysics, Yale University, PO Box 208109, New Haven, Connecticut 06520-8109, USA  
(tanya.lyubetskaya@yale.edu)

**ABSTRACT** The effects of metamorphic reactions on the thermal structure of a collisional overthrust setting are examined via forward numerical modelling. The 2D model is used to explore feedbacks between the thermal structure and exhumation history of a collisional terrane and the metamorphic reaction progress. The results for average values of crustal and mantle heat production in a model with metapelitic crust composition predict a 25–40 °C decrease in metamorphic peak temperatures due to dehydration reactions; the maximum difference between the  $P$ – $T$ – $t$  paths of reacting and non-reacting rocks is 35–45 °C. The timing of the thermal peak is delayed by 2–4 Myr, whereas pressure at peak temperature conditions is decreased by more than 0.2 GPa. The changes in temperature and pressure caused by reaction may lead to considerable differences in prograde reaction pathways; the consumption of heat during dehydration may produce greenschist facies mineral assemblages in rocks that would have otherwise attained amphibolite facies conditions in the absence of reaction enthalpy. The above effects, although significant, are produced by relatively limited metamorphic reaction which liberates only half of the water available for dehydration over the lifetime of the prograde metamorphism. The limited reaction is due to the lack of heat in a model with the average thermal structure and relatively fast erosion, a common outcome in the numerical modelling of Barrovian metamorphism. This problem is typically resolved by invoking additional heat sources, such as high radiogenic heat production, elevated mantle heating or magmatism. Several models are tested that incorporate additional radiogenic heat sources; the elevated heating rates lead to stronger reaction and correspondingly larger thermal effects of metamorphism. The drop in peak temperatures may exceed 45 °C, the maximum temperature differences between the reacting and non-reacting  $P$ – $T$ – $t$  paths may reach 60 °C, and pressure at peak temperature conditions is decreased by more than 0.2 GPa. Field observations suggest that devolatilization of metacarbonate rocks can also exert controls on metamorphic temperatures. Enthalpies were calculated for the reaction progress recorded by metacarbonate rocks in Vermont, and were used in models that include a layer of mixed metapelite–metacarbonate composition. A model with the average thermal structure and erosion rate of 1 mm year<sup>-1</sup> can provide only half of the heat required to drive decarbonation reactions in a 10 km thick mid-crustal layer containing 50 wt% of metacarbonate rock. Models with elevated heating rates, on the other hand, facilitated intensive devolatilization of the metacarbonate-bearing layer. The reactions resulted in considerable changes in the model  $P$ – $T$ – $t$  paths and ~60 °C drop in metamorphic peak temperatures. Our results suggest that metamorphic reactions can play an important role in the thermal evolution of collisional settings and are likely to noticeably affect metamorphic  $P$ – $T$ – $t$  paths, peak metamorphic conditions and crustal geotherms. Decarbonation reactions in metacarbonate rocks may lead to even larger effects than those observed for metapelitic rocks. Endothermic effects of prograde reactions may be especially important in collisional settings containing additional heat sources and thus may pose further challenges for the ‘missing heat’ problem of Barrovian metamorphism.

**Key words:** Barrovian; enthalpy; metacarbonate rocks; metamorphic reactions; thermal budget.

## INTRODUCTION

The thermal evolution of continental crust during orogenic collision and overthrusting has long been a subject of intensive research (e.g. Bird *et al.*, 1975; England & Thompson, 1984; Jamieson *et al.*, 2002). A common feature of orogenic belts is the presence of high-temperature (600–700 °C) metamorphic mineral assemblages at crustal depths of 20–30 km (~0.5–

0.8 GPa), and in some cases the products of melting associated with peak metamorphic conditions. Studies using numerical models of continental collision, however, have shown that it is difficult to reproduce temperatures in excess of 600 °C for common values of crustal heat production, convergence and surface erosion rates (e.g. Jamieson *et al.*, 1998). A variety of studies using numerical models have examined the potential sources and sinks of heat during collisional

orogeny, including: (1) high levels of transient heat flow from the asthenosphere (Bird, 1978; De Yoreo *et al.*, 1991; Bodorkos *et al.*, 2002); (2) shear heating within fault zones (Bird *et al.*, 1975; Molnar & England, 1990); (3) viscous heating (e.g. Burg & Gerya, 2005); (4) redistribution and accretion of heat-producing elements during deformation (Royden, 1993; Huerta *et al.*, 1996, 1998); (5) heat advection by fluid (Chamberlain & Rumble, 1989; Peacock, 1989); (6) magmatism and, in some cases, the associated metamorphic fluid flow (Lux *et al.*, 1986; Hanson & Barton, 1989; Baxter *et al.*, 2002; Ague & Baxter, 2007). The heat of metamorphic hydration and dehydration reactions, however, is almost always neglected in numerical calculations of the thermal budgets of collisional zones.

The potential importance of the heat produced and consumed during metamorphism in the total heat budget of subduction and collisional zones was first recognized in the late 1970s based on the first-order estimates made by Anderson *et al.* (1976). Anderson *et al.* (1978) suggested that the dehydration of the water-rich oceanic crust in the downgoing slab may consume 30–100% of the frictional heat generated along the slip zone. Walther & Orville (1982) stressed the significance of the thermal effect of reactions during regional metamorphism of pelitic terranes, and Peacock (1987) proposed that the thermal evolution of subduction zones may be considerably delayed by dehydration of oceanic crust and hydration within the hanging wall of the thrust. Later works by Peacock (1990, 1991), however, concluded that low-temperature dehydration in the subduction zone may cause only very small ( $\sim 5$  °C) temperature perturbations in the reacting rock. Nonetheless, field observations by Ferry (1980, 1983) suggested that mineral reactions may have exerted considerable controls on the heat budget of metamorphism in south-central Maine.

The very few attempts to include the effect of reactions in numerical models of collisional zones have led to somewhat contradictory conclusions. Whereas Peacock (1989) stated that dehydration reactions in the overthrust model may decrease the temperature at the base of the crust by more than 50 °C and retard the thermal evolution of thickened crust by several million years, Connolly & Thompson (1989) argued that the reduction in temperature in an overthrust zone produced by metamorphic reaction is  $< 40$  °C, and the timing or depth at which the peak temperatures are reached are not affected by metamorphic reactions in any noteworthy way. In a more recent work by Gerya *et al.* (2002) the thermal effect of the prograde phase transformations in a 1D overthrust model with dioritic and granodioritic crust composition was found to be about 10–20 °C. On the other hand, Haack & Zimmermann (1996) argued that retrograde hydration reactions may provide a noticeable source of heat in crustal rocks.

This paper revisits the problem of the thermal effects produced by metamorphic reactions in a collisional overthrust setting. A 2D thermal model is used to compute the thermal history of an overthrust terrane after the end of collision. The forward modelling approach allows us to analyse the temporal evolution of temperature, pressure, metamorphic reaction rates and mineral water supply within the reacting rocks, and to examine the relationships and feedbacks between these variables and the many parameters that control the  $P$ – $T$  evolution of a collision zone. Such controlling parameters, among others, include exhumation rates and crustal and mantle heat sources. The model incorporates several phenomena that have not received much attention in previous models of regional metamorphism. Thermal budgets are assessed not only of hydration and dehydration reactions in metapelites but also of solid–solid reactions and dehydration and decarbonation reactions in mixed metapelite–metacarbonate rocks. We also attempt to employ available field observations on metamorphic reactions as a benchmark for some of the numerical models. Finally, the thermal effects of metamorphic reactions are considered in a larger context of the heat budget of collisional orogens with Barrovian  $P$ – $T$  patterns, and evaluate the potential effect of increased heating rates on the progress and heat budget of regional metamorphism.

## MODEL FORMULATION

The 2D numerical model simulates the thermal evolution of an overthrust setting after the completion of plate convergence. The orogen geometry is represented with a thrust sheet of an average crustal thickness (35 km) that is emplaced over the distance of 120 km from the left boundary, the upper 5 km elevated above the surface comprising the topography. The emplaced section tapers off between 60 and 120 km from the left boundary. The vertical dimension of the model is 100 km, and the horizontal dimension is 240 km (Fig. 1; see Appendix for details of the model formulation).

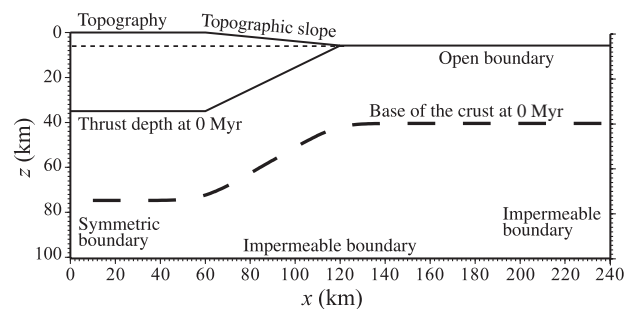


**Fig. 1.** Schematic geometry of the model and boundary conditions. The depths of the fault and of the base of the crust are for the initial state of the model. The base of the crust at the end of the simulation is at 35 km depth. The topography of the model is assumed to be steady-state.

The model is based on the assumption that plate convergence and thrusting are finished by the beginning of the simulation. The horizontal advection of rock as well as rock deformation are therefore not included in this treatment, which is focused primarily on thermal perturbations produced by metamorphic reactions. Potential effects of heat sources associated with these processes (e.g. shear stresses along the fault or viscous dissipation) will be reviewed below.

The thermal evolution of a model crustal section is calculated with the conservation of energy law:

$$\rho_m C_p^m \frac{\partial T}{\partial t} = \nabla(k_c \nabla T) - C_p^f \nabla \cdot (uT) - \rho_m C_p^m U \frac{\partial T}{\partial z} + A - Q_r.$$

The equation includes thermal conduction (first term on the right-hand side), advection of heat by fluid and exhuming rock (second and third terms), radiogenic heating (fourth term) and latent heat of metamorphic reactions (the last term on the right-hand side; see Table 1 for the list of variables). The latent heats of fusion and crystallization are not taken into account in this treatment. The effect of the fluid flow and of the temperature-dependent rock conductivity on the model thermal evolution are tested with a series of simulations (Table 3, see Appendix for details). Given our initial and boundary conditions, these effects are found to be minor in the context of large possible variations in crustal thermal structure and exhumation history. Thus, most of our models neglect the advection of heat by fluid flow and use the constant value of thermal conductivity,  $k_c = 2.25 \text{ W m}^{-2}$ , throughout the crust (Table 3).

**Table 1.** Notation and typical values used in modelling.

Variable	Value	Unit
$A$	$3 \times 10^{-6}$	$\text{W m}^{-3}$
$C_p^f$	1046	$\text{J kg}^{-1} \text{K}^{-1}$
$C_p^m$	880	$\text{J kg}^{-1} \text{K}^{-1}$
$g$	9.8	$\text{m s}^{-2}$
$k_c$	2.25	$\text{W m}^{-1} \text{K}^{-1}$
$k_\phi$	$10^{-19}$	$\text{m}^2$
$m$		$\text{mol l}^{-1}$
$m_{\text{H}_2\text{O}}$	$18 \times 10^{-3}$	$\text{kg mol}^{-1}$
$M_{\text{H}_2\text{O}}$		wt%
$n$		
$P$		Pa
$q_b$	$30 \times 10^{-3}$	$\text{W m}^{-2}$
$Q_r$		$\text{J m}^{-3}$
$T$		K
$T_p$		$^{\circ}\text{C}$
$T_s$	0	$^{\circ}\text{C}$
$u$		$\text{kg m}^{-2} \text{s}^{-1}$
$U$	0.5, 1	$\text{mm year}^{-1}$
$X_f$	0.05	$\text{kg kg}^{-1}$
$z_A$	$10^4$	m
$\Delta H$		
$\Delta T$	550	$^{\circ}\text{C}$
$\mu_f$	$1.15 \times 10^{-4}$	Pa s
$\phi$	0.0005	$\text{m}^3 \text{m}^{-3}$
$\rho$		$\text{kg m}^{-3}$
$\rho_m$	2800	$\text{kg m}^{-3}$
$\xi$		$\text{mol l}^{-1}$

The energy equation is solved with the finite difference method, using a grid size of 0.5 km in the  $z$  dimension and 2 km in the  $x$  dimension together with a time step of 0.01 Myr. The simulation time for each model is determined by the time required for exhuming 35 km of the crustal rock in the thrust segment of the model. For typical erosion rates considered in this work, 1 and 0.5  $\text{mm year}^{-1}$ , the simulation times are correspondingly 35 and 70 Myr. The topography is assumed to be steady-state and is not levelled with exhumation.

Although metamorphic reaction rates are generally dependent on a large number of factors, such as surface reaction mechanisms, the process of product nucleation, or mass transport (e.g. Ague, 1998), theoretical analysis (e.g. Ridley, 1986; Lutge *et al.*, 2004) and field observations (e.g. Ferry, 1983) indicate that the major control on metamorphic reactions is likely to be the rate at which heat is supplied or withdrawn from the system. Even in the case of nucleation-related thermal overstepping, the input of heat is the ultimate driving force of metamorphic reaction (e.g. Wilbur & Ague, 2006; Pattison & Tinkham, 2009). The earliest models that incorporated the heat of reaction in thermal calculations did so by adjusting thermal diffusivity and an effective heat capacity for rocks undergoing reaction (e.g. Hanson & Barton, 1989; Peacock, 1989). In the model of Connolly & Thompson (1989) the heat of reaction term is introduced directly into the energy conservation equation, but is assumed to be independent of the metamorphic reaction rates. Our work also includes the heat of reaction term,  $Q_r$ , in the energy equation; the term, however, is proportional to the rate of the overall temperature change within a rock parcel (e.g. Hanson, 1997):

$$Q_r = \frac{\Delta H}{m_{\text{H}_2\text{O}}} \frac{X_f \rho_m}{\Delta T} \frac{\partial T}{\partial t},$$

where  $\Delta H$  is the latent heat of reaction and  $X_f$  is the total amount of fluid with molar weight  $m_{\text{H}_2\text{O}}$  released/absorbed by the rock with density  $\rho_m$  over the characteristic temperature interval for reaction,  $\Delta T$ . The sign of the temperature change determines the direction in which hydration/dehydration reactions proceed in a particular rock parcel: endothermic dehydration reactions require the addition of heat, i.e.  $\partial T / \partial t > 0$ , whereas exothermic hydration reactions occur when  $\partial T / \partial t < 0$ .

The rock composition in our default model is assumed to be an average metapelitic rock (see below). In addition, metamorphic reactions are also considered in rock packages with variable lithologies, consisting of alternating layers of metapelites and metacarbonates.

### Metamorphic reactions in metapelitic rock

Pseudosection calculations to assess water loss from metapelites were done using Theriak Domino (version 150508; <http://titan.minpet.unibas.ch/minpet/theriak/>)

theruser.html). Results for typical metapelitic compositions, such as those described by Ague (1994) or Powell *et al.* (1998), indicate loss of ~3.75 to 6.5 wt% (~5.86–10.15 mol l<sup>-1</sup>) of water between 200 and 750 °C, with the largest fraction of the loss occurring between roughly 400 and 650 °C. Consequently, a representative value of 5 wt% (7.81 mol l<sup>-1</sup>) loss of water in dehydration reactions is modelled over the temperature interval of 200–750 °C. Reaction is assumed to be fastest at temperatures between 400 and 650 °C, with the rate of fluid production corresponding to 3 wt% (4.69 mol l<sup>-1</sup>) water loss over 250 °C or 0.012 wt% °C<sup>-1</sup>. Reaction rates for temperatures from 650 to 750 °C and from 200 to 400 °C are 0.01 wt% °C<sup>-1</sup> and 0.005 wt% °C<sup>-1</sup> respectively. The intensive reaction between 400 and 650 °C corresponds largely to the breakdown of chlorite and, to a lesser degree, mica. This devolatilization amounts to 4.7 mol of H<sub>2</sub>O lost per litre of rock (neglecting any rock volume changes). Field studies document similar values. For example, the Ferry (1994) study of metapelites and metasandstones of the Waits River Formation showed that the rocks lost, on average, 4.25 mol total fluid per litre rock over the 475–550 °C range. If the rocks had been heated to 650 °C, the total amount of volatiles lost would almost certainly have been greater. For another example, Pattison (2006) found that the average fluid loss from metapelitic rocks reacting between about 550 and 625 °C was 2.89 wt% (4.5 mol l<sup>-1</sup>). The percentage volatile loss in our model is greatest between 400 and 650 °C in order to better reflect metamorphic processes, but we note that models with a uniform 5 wt% water loss from 200 to 750 °C produce very similar results.

Metamorphic reactions may only occur in the rocks that contain a supply of fluid in the form of chemically bound volatiles (in case of dehydration reactions) or pore fluid (in case of hydration). The initial water content in crustal rocks is modelled as a function of the initial temperature distribution, based on the 5 wt% upper limit for the bound water supply. Rocks at temperatures below 400 °C are assumed to be fully hydrated; the water content of rocks at >400 °C drops linearly from 5 wt% to 0 over the temperature interval of 300 °C. In our default model, the porous space of crustal rocks is assumed to be always filled with fluid available for hydration reactions; hydration is allowed to proceed until the upper limit for the bound water content, 5 wt%, is attained. In addition, an alternative scenario is considered in which no hydration reactions occur during rock cooling (see Table 3 for the list of simulations).

The enthalpy changes for a number of common reactions at a representative pressure of 0.8 GPa are shown in Table 2. Enthalpy changes for reactions proceeding at temperatures less than about 400–450 °C, such as pyrophyllite dehydration, tend to be smaller than enthalpy changes for higher temperature reactions. For a representative suite of 20 dehydration

**Table 2.** Representative metamorphic reactions in metapelites.

Reaction	$\Delta H$ (kJ mol <sup>-1</sup> )
Pyrophyllite = kyanite + 3 quartz + H <sub>2</sub> O	36.7 (B91) 39.5 (HP98)
2 diaspore = corundum + H <sub>2</sub> O	51.3 (B91) 53.3 (HP98)
3 clinocllore + muscovite + 3 quartz =	57.6 (B91) 58.5 (HP98)
4 pyrope + phlogopite + 12 H <sub>2</sub> O	
7 quartz + 23 Fe-chloritoid = 2 Fe-staurolite	63.8 (HP98)
+ 5 almandine + 19 H <sub>2</sub> O	
Muscovite + quartz = K-feldspar + Al <sub>2</sub> SiO <sub>5</sub> + H <sub>2</sub> O	54.0 (B91) 64.4 (HP98)
Aragonite = calcite	3.7 (HP98)
Kyanite = sillimanite	11.3 (B91) 11.7 (HP98)
Alpha-quartz = beta-quartz	11.6 (B91)
Almandine + phlogopite = pyrope + annite	52.1 (FS78)

$\Delta H$  values are per mole of fluid for dehydration reactions, or per mole of reaction as written for solid–solid reactions. Thermodynamic data from Berman (1991), Holland & Powell (1998) and Ferry & Spear (1978).

reactions, an average of  $35.4 \pm 8.4$  kJ mol<sup>-1</sup> ( $2\sigma$ ) per mole H<sub>2</sub>O released is calculated for reactions proceeding at  $\leq 420$  °C, and  $56.4 \pm 7.2$  kJ mol<sup>-1</sup> for higher temperature reactions. As  $\Delta H$  values are relatively insensitive to pressure, the above values are used throughout the model crust.

Because dehydration reactions consume the largest proportion of heat, solid–solid reactions are generally neglected in energy conservation expressions. However, prograde solid–solid reactions are nearly all endothermic and may play a role analogous to that of dehydration reactions in the total crustal heat budget. For example, the transformation of kyanite to sillimanite consumes in excess of 11 kJ mol<sup>-1</sup> (Table 2). Other examples include the alpha–beta quartz transition and the aragonite–calcite transition. Prograde Fe–Mg exchange should also be considered. A common reaction is the garnet–biotite thermometer, which has a large  $\Delta H = 52.108$  kJ mol<sup>-1</sup> (Ferry & Spear, 1978). Even a marble that undergoes no devolatilization will consume heat owing to the aragonite–calcite transition. A pure marble would consume over 100 kJ l<sup>-1</sup>; this amount of heat is larger than that required to drive the loss of 1 wt% water by dehydration.

Let us consider the heat consumed by simple solid–solid reactions such as those in Table 2, in a rock that contains 15 vol% kyanite, 30% quartz and 10% garnet; the remainder would include other minerals such as sheet silicates and plagioclase. On heating of the rock to 750 °C at 0.8 GPa, the transitions among the Al<sub>2</sub>SiO<sub>5</sub> and SiO<sub>2</sub> polymorphs will consume 40 and 22 kJ l<sup>-1</sup> respectively. The calculation for Fe–Mg exchange is more uncertain as it will vary with bulk rock composition and the range over which garnet and biotite react, but the result should be roughly in the range of 15 kJ l<sup>-1</sup>. In our model, a rock will lose 3.76 wt% water over the temperature interval 420–750 °C, with a heat consumption of  $\sim 322$  kJ l<sup>-1</sup> assuming  $\Delta H = 55$  kJ mol<sup>-1</sup>. Adding the contributions of the solid–solid reactions increases the value of consumed heat considerably to  $\sim 397$  kJ l<sup>-1</sup>. We can solve for the average amount of heat consumed per mole of water released using this total heat consumption value. The

**Table 3.** Numerical experiments and results

Model	Thermal structure	$U$ (mm yr <sup>-1</sup> )	For a rock initially at 50 km depth				For a rock initially at 60 km depth			
			$T_p \Delta H = 0$	$T_p \Delta H < > 0$	$\Delta T_p$	max $\Delta T$	$T_p \Delta H = 0$	$T_p \Delta H < > 0$	$\Delta T_p$	max $\Delta T$
Reference model	standard <sup>1</sup>	1.0	570	541 (539)	29 (31)	34 (35)	660	634 (631)	26 (29)	36 (36)
		0.5	632	602 (600)	30 (32)	41 (41)	729	704 (701)	25 (28)	42 (42)
		1.0 after 10Ma	634	596 (594)	38 (40)	45 (46)	720	688 (684)	32 (36)	46 (46)
$T$ -dependent $k_c$	standard	1.0	566	536	30	34	666	638	28	37
		0.5	634	601	33	42	748	722	26	44
		1.0 after 10Ma	635	595	40	46	733	699	34	47
Fluid flow	standard	1.0	570	545 (545)	25 (26)	27 (28)	660	639 (637)	21 (23)	27 (27)
Radiogenic heat source <sup>2</sup>	$A_{en} = 3\mu\text{W m}^{-3}$	1.0	639	602 (598)	37 (41)	46 (47)	722	690 (685)	32 (37)	46 (48)
	$A_{en} = 4\mu\text{W m}^{-3}$	1.0	707	661 (657)	46 (50)	58 (59)	781	744 (738)	37 (43)	57 (58)
Elevated basal heat flow	$q_b = 60 \text{ mW m}^{-2}$	1.0	601	568	33	39	734	708	26	42
	$q_b = 90 \text{ mW m}^{-2}$	1.0	632	597	35	45	800	774	26	48
50%-metacarbonate layer (at $z = 35\text{-}45$ km)	standard	1.0	570	545 (540)	25 (30)	28 (33)	660	639 (632)	21 (28)	28 (35)
		1.0	570	531 (531)	39 (39)	41 (42)	660	627 (635)	33 (35)	40 (41)
		0.5	632	588 (586)	44 (46)	60 (61)	729	695 (693)	34 (36)	54 (55)
(at $z = 45\text{-}55$ km; alternative <sup>3</sup> )	standard	0.5	632	583	49	62	729	693	36	55
		1.0	570	521 (519)	49 (51)	50 (52)	660	617 (613)	43 (47)	62 (63)
20%-metacarbonate layer (at $z = 45\text{-}55$ km)	standard	1.0	570	536	34	38	660	631	29	39
		0.5	632	597	35	50	729	701	28	48
80%-metacarbonate layer (at $z = 45\text{-}55$ km)	standard	1.0	570	530	40	43	660	625	35	41
		0.5	632	582	50	66	729	691	38	59
50%-metacarbonate layer (at $z = 45\text{-}55$ km)	$A_{en} = 4\mu\text{W m}^{-3}$	1.0	707	646 (642)	61 (65)	98 (98)	781	732 (727)	49 (54)	78 (78)
20%-metacarbonate layer (at $z = 45\text{-}55$ km)	$A_{en} = 4\mu\text{W m}^{-3}$	1.0	707	655 (652)	52 (55)	75 (77)	781	739 (734)	42 (47)	66 (67)
80%-metacarbonate layer (at $z = 45\text{-}55$ km)	$A_{en} = 4\mu\text{W m}^{-3}$	1.0	707	636 (631)	71 (76)	110 (110)	781	725 (721)	56 (60)	85 (86)

All temperatures are in °C. For comparison, results for models without metamorphic reactions ( $\Delta H = 0$ ) and with prograde and retrograde reaction ( $\Delta H < > 0$ ) are shown. When available, the results for models with prograde reactions only ( $\Delta H > 0$ ) are shown in parenthesis.  $\Delta T_p$  denotes the difference in peak temperatures,  $T_p$ , in the reacting and non-reacting models; max  $\Delta T$  is the maximum drop in temperature in the reacting model compared to the non-reacting case. Model thermal structures: <sup>1</sup>Basal heating  $q_b = 30 \text{ mW m}^{-2}$ ; surface radiogenic heat  $A = 3\mu\text{W m}^{-3}$ . <sup>2</sup>Contains a layer enriched in radiogenic elements at the initial depth 35–40 km. <sup>3</sup>Metacarbonate-bearing layer comprises ten alternating bands 1 km thick of pure metapelitic and metacarbonate composition.

result is  $\sim 68 \text{ kJ mol}^{-1}$ , significantly greater than the value of  $55 \text{ kJ mol}^{-1}$  for dehydration alone. Based on these results, a value of  $65 \text{ kJ mol}^{-1}$  is used as the effective latent heat of dehydration and solid–solid metamorphic reactions at temperatures above  $420 \text{ }^\circ\text{C}$ . This is the same as the average of the values used by Connolly & Thompson (1989) although no solid–solid reactions were considered in that work.

The above values of  $\Delta H$  are likely to be conservative estimates as many other reactions have not been considered, such as all the Fe–Mg exchanges among AFM phases (e.g. garnet, staurolite, chloritoid, biotite, chlorite, cordierite), Na–K exchange in white mica, and feldspar phase transitions. Furthermore, we do not include here the contributions of metacarbonate rocks, which in general have larger enthalpy changes per mole of fluid released than dehydration reactions (e.g. calcite + quartz = wollastonite +  $\text{CO}_2$ ;  $\sim 80 \text{ kJ mol}^{-1}$ ). The generally endothermic prograde reactions may also include heat of solution effects in fluids (e.g. the heat of mixing for  $\text{CO}_2\text{-H}_2\text{O}$  is non-ideal and positive). All these kinds of reactions could in fact contribute to the overall metamorphic budget. For lower temperatures (below  $420 \text{ }^\circ\text{C}$ )  $35 \text{ kJ mol}^{-1}$  is used as there are fewer phase transitions and solid solution effects at these conditions, and less heat is required to dehydrate the low- $T$  hydrous minerals.

Thermal overstepping due to kinetic barriers may affect some devolatilization and solid–solid transformations. Overstepping will delay the onset of reaction but, once reaction begins, the rates of reaction will in general be greater than for cases where overstepping is absent (e.g. Ague *et al.*, 1998; Wilbur & Ague, 2006). These greater rates are likely to lead to larger thermal effects for overstepped reactions because, as will be shown below, the heat budget of metamorphism is dependent on the rate of reaction. Overstepping, however, is not explicitly modelled in our work.

### Metamorphic reactions in metacarbonate rocks

In addition to our default models which use an average metapelitic crust composition, another case is considered which includes a layer rich in metacarbonate rocks. As was mentioned above, dehydration and decarbonation reactions in metacarbonate rocks may consume significant amounts of heat. In particular, the field study by Ferry (1983) reported local buffering of temperature by prograde metamorphic reactions within impure carbonate rock sequences in south-central Maine (Vassalboro Formation). These data provide unique first-hand information on the actual amount of heat that may be consumed during prograde metamorphism. Extensive metamorphic

reactions in metacarbonate-rich rocks in large areas of south-central Maine and eastern Vermont have been documented by later studies as well (e.g. Ferry, 1992, 1994). Field data from the Waits River Formation in Vermont are used to estimate the enthalpy of decarbonation reactions in metacarbonate rocks at different metamorphic conditions. The detailed descriptions of mineral reactions and the heat of reaction estimates are included in the Appendix, and only a short summary is given here.

There are four major groups of reactions that occurred in metacarbonate rocks within the temperature interval 500–580 °C: (1) transition from the ankerite–albite zone to the ankerite–oligoclase zone (equilibrium temperature  $T_{\text{eq}} = 500$  °C, heat of reaction  $Q_r = 8.8$  kJ l<sup>-1</sup>); (2) transition to the biotite zone ( $T_{\text{eq}} = 530$  °C,  $Q_r = 158.3$  kJ l<sup>-1</sup>); (3) transition to the amphibole zone ( $T_{\text{eq}} = 545$  °C,  $Q_r = 79.7$  kJ l<sup>-1</sup>); and (4) transition to the diopside zone ( $T_{\text{eq}} = 570$  °C,  $Q_r = 224.5$  kJ l<sup>-1</sup>). The total amount of heat consumed on the prograde heating of a metacarbonate rock from 500 to 580 °C is therefore  $Q_r = 470$  kJ l<sup>-1</sup>. These reactions are strongly driven by infiltration of rock by H<sub>2</sub>O fluid, rather than just heating of the rock as in the case of dehydration reactions in metapelites. For this reason the metacarbonate reaction progress is modelled in a different way than in the case of metapelites.

Transport of H<sub>2</sub>O from dehydrating metapelitic rocks into metacarbonate rocks by flow, diffusion and mechanical dispersion is assumed to be capable of driving each of the four major infiltration-dependent reactions when the rock attains the corresponding equilibrium temperature ( $T_{\text{eq}} = 500, 530, 545$  or 570 °C). The extent of reaction in each case is determined by the amount of heat that is available for decarbonation in a model rock. Numerically, the temperature within a reacting rock parcel is maintained at the corresponding  $T_{\text{eq}}$  value until the amount of heat required for such thermal buffering exceeds the characteristic  $Q_r$  value for this reaction. The equilibrium conditions for these reactions are likely to extend over temperature intervals (e.g. Ague, 2000), and our use of the constant temperature values for  $T_{\text{eq}}$  is clearly a simplification. It is, however, unlikely to significantly affect our results as the equilibrium temperature intervals in the above reactions (15–30 °C) are relatively narrow in comparison with the total temperature variations in the system. The above approach does not take into account the influence of changes in pressure on reaction progress. To minimize these effects, the metacarbonate-bearing layer in most of our models reacts in the pressure interval that encompasses the geobarometry estimates for metacarbonate rocks that were used to compute our heat of reaction values,  $Q_r$  (Ferry, 1992).

The compositions of the rock packages described by Ferry (1992, 1994) are heterogeneous; for example, the amount of metacarbonate rocks varies from 20–50%

in the western part of the Waits River Formation (east-central Vermont) to 50–80% in the east. The packages are up to 60 km in lateral extent and at least 5 km thick in the mapped cross-sections (Doll *et al.*, 1961). Our models are meant to explore the effect of carbonate lithology on the thermal history of a metamorphosed terrane and include a single metapelite–metacarbonate layer with a 10 km thickness and lateral extent 30 km at different depths in the underthrust region of the model crustal section. Based on the field data, the rocks within this layer are assumed to be of mixed composition with metapelites and metacarbonates present in different proportions. Metamorphic reactions are modelled in the following way: reaction in metapelites proceeds continuously over the temperature interval 200–750 °C with the amount of produced (or consumed) fluid  $X_f$  weighted according to the proportion of metapelitic rocks in the layer. Reaction in metacarbonate rocks occurs at four discrete temperatures –  $T_{\text{eq}} = 500, 530, 545$  and 570 °C – on the prograde heating path of the rock; the corresponding heat of reaction values  $Q_r$  for each  $T_{\text{eq}}$  are weighted by the proportion of metacarbonates within the layer. This approach has been tested with an alternative scenario, in which the metacarbonate-bearing layer was composed of 10 alternating bands 1 km thick of pure metacarbonate and metapelite compositions. The results for this type of model were found to be very similar to the ones presented here (see Table 3 for details).

## RESULTS

### The effect of exhumation history on the reaction progress for the average thermal structure of a model crust

The distribution of mantle and crustal heat sources, i.e. basal heating and radiogenic heating, are fundamental controls on the subsequent thermal evolution of a model collision zone. The thermal structure of our reference model has a surface heat flow of 60 mW m<sup>-2</sup>, which is an average value for the mean surface heat flow in most of the geological provinces in the continental crust (30–90 mW m<sup>-2</sup>, Jaupart & Mareschal, 2003). The relative contributions of crust and mantle heat sources to the surface heat flow are uncertain and may only be inferred indirectly from geochemical data on the crustal content of heat-producing elements, and seismic velocities in the lower crust (e.g. Rudnick *et al.*, 1998). The heat flow from the mantle is generally estimated at 20–30 mW m<sup>-2</sup> in old stable regions of continental crust and up to 60 mW m<sup>-2</sup> in younger Phanerozoic provinces (Cermak, 1993), whereas the average surface radiogenic heat production on continents is generally within the range of 1–3.5 mW m<sup>-3</sup> (Sclater *et al.*, 1981; Jaupart & Mareschal, 2003). We use a mantle heat flow of 30 mW m<sup>-2</sup> and radiogenic heat production exponentially decreasing with depth with a characteristic length scale of 10 km and a

surface value of  $3 \times 10^{-6} \text{ W m}^{-3}$  as our reference thermal structure; these conservative values of crustal and mantle heat sources are commonly employed in numerical modelling (e.g. Peacock, 1989; Jamieson *et al.*, 1998). The above parameters result in a steady-state geotherm with a temperature of  $600 \text{ }^\circ\text{C}$  at the base of the crust (35 km depth). Within the thrust region, the instantaneous superposition of two steady-state geotherms would result in a sawtooth geotherm. It has long been suggested, however, that the sawtooth would require unrealistically high convergence rates (e.g. Shi & Wang, 1987). Therefore, the sawtooth temperature distribution is allowed to relax conductively for 0.5 Myr before the start of all simulations; this time interval is envisioned to encompass plate convergence and corresponding thermal accommodation during collision as these processes are not explicitly accounted for by our purely thermal model. The particular length of this time gap is dependent on the assumed rates of convergence, but our conclusions about the thermal consequences of reaction are unaffected.

Figure 2(a) compares the  $P$ - $T$ - $t$  paths computed for a crustal column located at  $x = 20 \text{ km}$  (model time points every 0.5 Myr) for the reference model with and without metamorphic reactions, for an exhumation rate of  $1 \text{ mm year}^{-1}$ . The  $P$ - $T$ - $t$  paths for rocks in the lower plate of the overthrust zone (initially below 35 km depth) exhibit the characteristic clockwise pattern: they undergo heating over the first 15–25 Myr due to the relaxation of the faulted geotherm, and subsequent cooling at 20–35 Myr as a result of exhumation into the shallower parts of the crust. Endothermic dehydration reactions in the heated rocks displace the  $P$ - $T$ - $t$  paths in the reacting model towards lower temperatures; at a given depth (or at a certain time in the exhumation history) the difference in rock temperatures between the reacting and non-reacting models may reach  $35 \text{ }^\circ\text{C}$  (Fig. 2c).

A considerable decrease in pressure along the heating path of metamorphism is another effect of dehydration reactions that is rarely or never discussed in the literature: in the reacting model a certain temperature is attained at a shallower depth and correspondingly lower pressure in comparison with the non-reacting case. The difference in pressure between the reacting and non-reacting models ( $\Delta P$ ) may exceed 0.2 GPa for underthrust rocks on their heating path (Fig. 2d), corresponding to a  $\sim 7 \text{ km}$  difference in depth. After the peak metamorphic temperature is attained, the difference in pressure becomes negative: i.e. in a reacting model a certain temperature is attained at a deeper level and correspondingly higher pressure in comparison with the non-reacting case. The peak metamorphic conditions for rocks in the reacting model are therefore transferred to lower pressures and shallower depths.

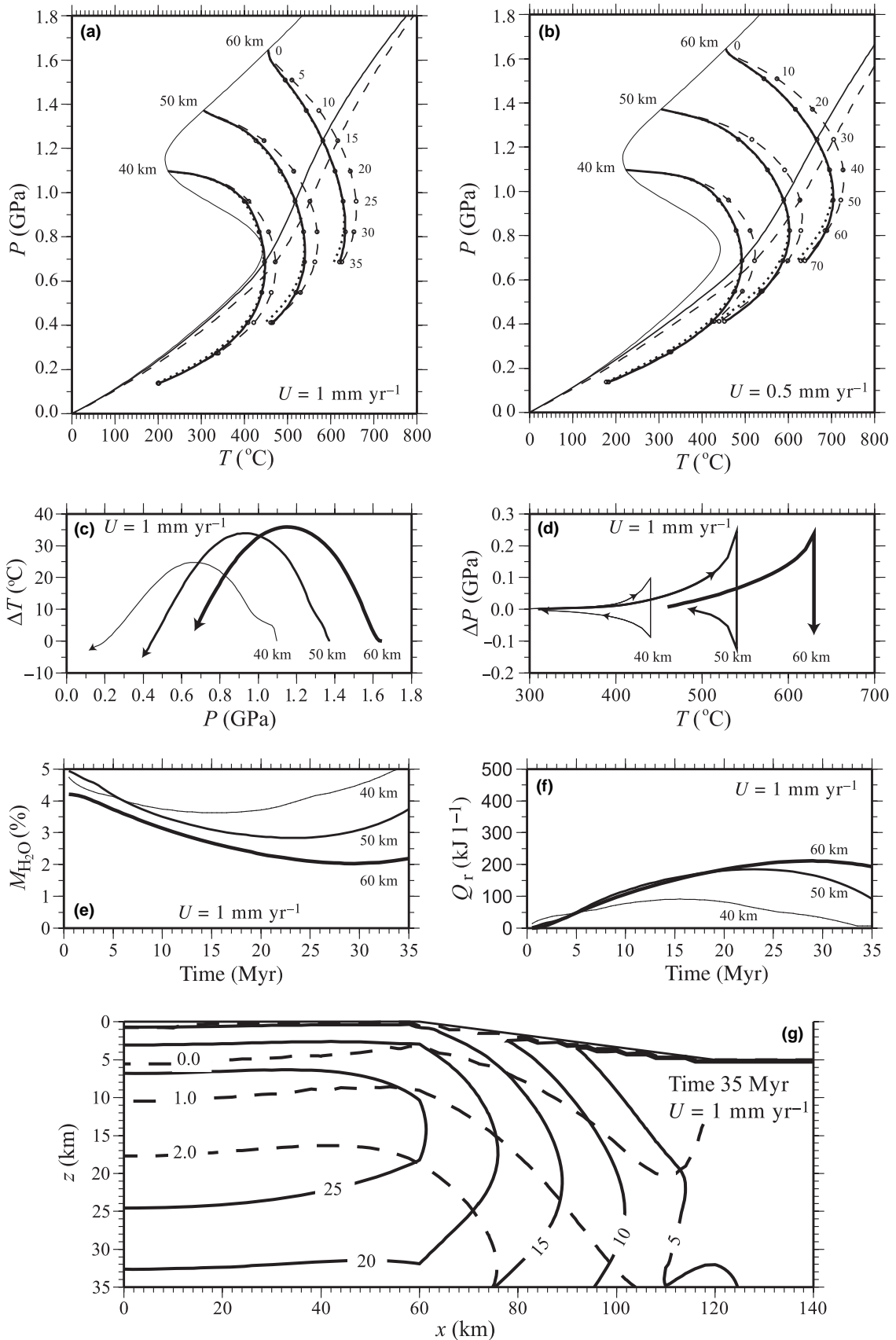
Figure 2(g) shows the 2D distribution of the difference between the peak metamorphic temperatures and

the time when these temperatures were attained for the reacting and non-reacting models at the end of simulation (35 Myr). For the parameter space used in this model, metamorphic reactions reduce peak temperatures by more than  $25 \text{ }^\circ\text{C}$  for rocks initially below 45 km depth, and the time at which the peak conditions were attained is delayed by more than 2 Myr. The above differences in  $P$ - $T$ - $t$  paths between the reacting and non-reacting models may be summarized in terms of the change in the deep crustal geotherm due to hydration reactions at 15–25 Myr of the thrust evolution. At about 45 km the non-reacting model geotherm of  $6.7 \text{ }^\circ\text{C m}^{-1}$  is increased to  $7.0$ – $7.1 \text{ }^\circ\text{C m}^{-1}$  in the reacting model (Fig. 2a).

The release of chemical energy due to hydration on the cooling path of exhuming rock results in a slight increase in rock temperatures in the reacting model relative to the non-reacting case. As a result, the reacting and non-reacting  $P$ - $T$ - $t$  paths that diverge in the first 15–25 Myr due to dehydration reactions tend to converge again near the end of the model evolution (Fig. 2a,b). An alternative model in which no hydration reactions occur during rock cooling has lower temperatures in comparison with the non-reacting model even at the end of the simulation. The peak metamorphic temperatures in this model are reduced by an additional 2–5  $^\circ\text{C}$  (Table 3). Conversely, the time delay in the attainment of the peak conditions in this model is almost twice as short as in the one with hydration reaction allowed (about 1.5 Myr for deep rocks, Fig. 2a).

The effect of the latent heat of reaction on the thermal structure in the above model (Fig. 2a) is not very strong compared to the total thermal variations within the model; in this case, however, the potential of metamorphic reactions to control the temperature is far from being fully realized. By the end of the 35 Myr of thrust evolution, most of the rocks in the lower plate have lost less than half of the water available for dehydration (Fig. 2e). Even the deepest rocks that underwent the greatest dehydration retained 1.5–2 wt% of their water by the end of the prograde reaction path. First-order calculations suggest that metamorphic reactions having the parameters used in our modelling may potentially consume up to  $450 \text{ kJ l}^{-1}$  of heat. In the above model, the value of cumulative heat of reaction,  $Q_r$ , for the deepest rocks that underwent the most dehydration, is just above  $210 \text{ kJ l}^{-1}$  (Fig. 2f). The limited reaction progress is the consequence of relatively slow rates of temperature increase in this model with average crustal and mantle heat production. Only the very deepest rocks (below 55 km at the onset of the thrust evolution) attain temperatures in excess of  $600 \text{ }^\circ\text{C}$  (but below  $700 \text{ }^\circ\text{C}$ ) during 35 Myr of the thrust evolution (Fig. 2a). Such  $P$ - $T$ - $t$  paths are considered unrealistically cold in comparison with the field thermobarometry data for many convergent orogens (e.g. Jamieson *et al.*, 1998; Burg & Gerya, 2005).

Lower erosion rates (e.g.  $0.5 \text{ mm year}^{-1}$  over 70 Myr of thrust evolution; Fig. 2b) result in an



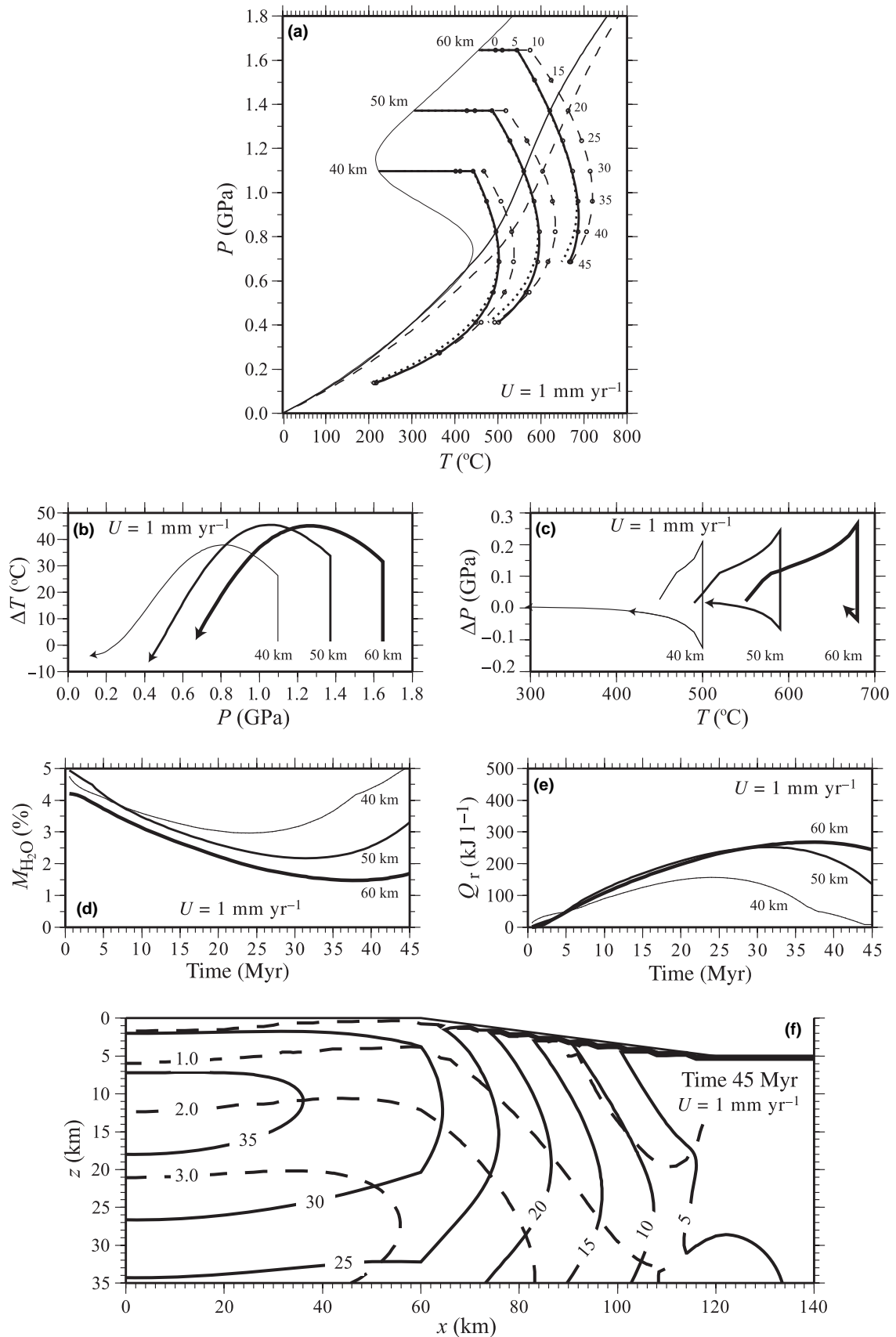
overall increase in rock temperatures because longer exhumation histories allow more time for the production of radiogenic heat within the lower plate of the thrust. They also allow more time for metamorphic reaction, and the amount of fluid that is extracted from deep rock at the end of the heating phase is increased by more than 0.5 wt% compared to the model with faster erosion. The amount of fluid consumed by rock on the cooling path is correspondingly elevated. However, because the rates of heating, the corresponding rates of metamorphic reaction and the rates of heat consumption by metamorphism in this model are approximately the same as in the case with faster erosion (albeit acting over longer time), the total effect of reaction on rock temperatures is only slightly larger than that in a model with an erosion rate of  $1 \text{ mm year}^{-1}$ . The maximum drop in metamorphic temperatures along the  $P$ - $T$ - $t$  paths is  $\sim 40^\circ\text{C}$ , and peak temperatures are decreased by about  $30^\circ\text{C}$  (Table 2). The delay in the peak temperature attainment, however, is considerably increased to more than 4 Myr for most of the rock below the thrust fault and more than 4.5 Myr for the deepest rocks; this reflects the twofold increase in the time-scale of exhumation (Fig. 2b).

A delay of several million years between the thrusting event and the onset of erosion also leads to increased temperatures in an overthrust model with standard thermal structure. Delays of 10 and 20 Myr have been considered in numerical modelling by England & Thompson (1984) and Connolly & Thompson (1989) based on the tectonic history of the Alpine chain (e.g. Richardson & England, 1979). Figure 3(a) presents the  $P$ - $T$ - $t$  paths for a model with an erosion rate of  $1 \text{ mm year}^{-1}$  initiated at 10 Myr after the start of the simulation. The peak temperatures for the deepest rocks in the non-reacting model are above  $700^\circ\text{C}$ ; the drop in peak temperatures due to dehydration reactions may exceed  $35^\circ\text{C}$ , and the maximum temperature decrease at constant pressure is  $45^\circ\text{C}$  (Fig. 3d). The 30% increase in the effect of reaction in this model in comparison with the standard model (i.e. from 29 to  $38^\circ\text{C}$  at 50 km, Table 3) is the result of the 10 Myr longer heating history of rocks in the underthrust zone. This leads to elevated fluid production and cumulative heat of reaction over a relatively short time-scale (Fig. 3d,e; compare with

Fig. 2e,f). Still, even in this scenario, metamorphic reactions extract only part of the water available for dehydration, and a considerable amount of water (on average 1.5–2 wt% in the underthrust zone) is retained in deep rocks at the end of the exhumation history.

The models discussed so far do not take into account the advection of heat by fluid flow and neglect the temperature dependence of thermal conductivity of crustal rocks. To test the potential effect that these limitations may have on the metamorphic thermal budget of our models, a number of supplementary simulations were run (see Table 3 for the full list of calculations). The dependence of rock conductivity  $k_c$  on temperature is formulated based on the relationships suggested by Gerya *et al.* (2002) for a dioritic composition within the crust and an ultramafic composition within the mantle section of the model (see Appendix). Figure 4(a) shows the results for a model identical to the reference case (Fig. 1a) but with variable  $k_c$ . The  $P$ - $T$ - $t$  paths have slightly different curvature reflecting the drop in  $k_c$  from about  $2.7 \text{ W m}^{-1} \text{ K}^{-1}$  at the surface to as low as  $1.4 \text{ W m}^{-1} \text{ K}^{-1}$  at the base of the model. A small increase in the temperature of the deep crust in this model in comparison with the fixed  $k_c$  case leads to slightly elevated reaction rates and to an additional  $1$ – $3^\circ\text{C}$  drop in model peak temperatures due to dehydration reactions. Other simulations with variable  $k_c$  and different erosion rates (Table 3) produce similar results. Despite some differences in the form of the  $P$ - $T$ - $t$  paths and peak temperature values, the drop in peak temperature caused by dehydration is only  $3$ – $4^\circ\text{C}$  larger than that for models with constant  $k_c$ . On the other hand, our neglect of heat advection by fluid in the reference models discussed above (Figs 2 & 3), is likely to result in a slight overestimate of the effect of reaction in the deepest rocks. Our model of fluid flow in the collisional setting predicts a  $4$ – $5^\circ\text{C}$  smaller decrease in peak metamorphic temperatures due to reaction, in comparison with our default model (Fig. 4b, Table 3). This estimate is likely to be an upper limit for the effect of fluid flow on the thermal evolution of the collisional setting in the parameter space of our model, as this formulation neglects rock deformation and porosity evolution and therefore maximizes deep crustal fluid flux (Lyubetskaya & Ague, 2009). As variable rock conductivity and heat

**Fig. 2.** Model results for average values of radiogenic heat production and basal heating. (a)  $P$ - $T$ - $t$  paths for rocks at erosion rate of  $1 \text{ mm year}^{-1}$  are shown with thick lines; dashed for the no reaction case ( $\Delta H = 0$ ), dotted for prograde reaction ( $\Delta H > 0$ ), solid for prograde and retrograde reaction ( $\Delta H \leq 0$ ). The model  $P$ - $T$ - $t$  paths in this and subsequent figures are computed for a crustal column located at  $x = 20 \text{ km}$ ; model time points are plotted every 0.5 Myr for models with erosion rate  $1 \text{ mm year}^{-1}$ , and every 1 Myr for erosion rate  $0.5 \text{ mm year}^{-1}$ . Crustal geotherms at 0 and 15 Myr are shown with thin lines; dashed for no reaction case, solid for prograde and retrograde reaction. (b) Same as (a), for erosion rate of  $0.5 \text{ mm year}^{-1}$ . (c) Temperature difference at constant pressure between reacting ( $\Delta H \leq 0$ ) and non-reacting rocks, erosion rate  $1 \text{ mm year}^{-1}$ . (d) Pressure difference at constant temperature between reacting ( $\Delta H \leq 0$ ) and non-reacting rocks, erosion rate  $1 \text{ mm year}^{-1}$ . (e) Temporal evolution of the fraction of bound water in crustal rocks for the model in (a),  $\Delta H \leq 0$ . (f) Temporal evolution of the cumulative heat of reaction for the model in (a),  $\Delta H \leq 0$ . (g) The 2D distribution of the difference in peak temperatures (solid lines,  $^\circ\text{C}$ ) and the timing of the thermal peak (dashed lines, Ma) between the reacting ( $\Delta H \leq 0$ ) and non-reacting model at the end of the simulation; erosion rate  $1 \text{ mm year}^{-1}$ .



advection by fluid have a relatively minor influence on the thermal effects of metamorphic reactions and, moreover, are likely to cancel each other's contributions, these effects are not taken into account in the subsequent numerical experiments.

### The effect of additional heat sources on the reaction progress

Thermomechanical models that try to reconstruct both the thermal evolution and the deformational history of collisional orogens (e.g. Huerta *et al.*, 1998; Jamieson *et al.*, 1998) have demonstrated that simple overthrusting of continental crust with average values of basal heating and radiogenic heat production does not usually provide the amount of heat needed to reproduce the  $P$ - $T$ - $t$  paths characteristic of typical orogens at realistic time-scales (i.e. Barrovian metamorphic conditions with temperatures above 650–700 °C at pressures below about 0.8 GPa in less than 50 Myr). A great number of studies have pointed to various heat sources that may help to resolve this 'missing heat' problem, including high levels of transient heat flow from the mantle, elevated radiogenic heat production, shear and viscous heating, and magmatism (e.g. Lux *et al.*, 1986; Barr *et al.*, 1991; De Yoreo *et al.*, 1991; Huerta *et al.*, 1998; Burg & Gerya, 2005; Ague & Baxter, 2007). There is still a considerable discussion about which of these heat sources, or a combination of several sources, may be responsible for Barrovian metamorphism in specific geological localities (e.g. Engi *et al.*, 2001; Goffé *et al.*, 2003), including the type locality in Scotland (Baxter *et al.*, 2002; Ague & Baxter, 2007). Whereas our models are not designed to specifically test any of the existing hypotheses, we can nevertheless make use of the concept of an additional heat source and examine the effect of enhanced heating rates on the thermal budget of metamorphic reactions.

Two scenarios are tested that promote fast heating rates in the model orogenic setting. The first one belongs to a large class of models that attribute the Barrovian  $P$ - $T$  conditions to enhanced radiogenic element content within the collisional zone. The elevated radiogenic heating in such scenarios may be the consequence of concentrated abundance of radiogenic elements in crustal sedimentary layers before the collision (e.g. Chamberlain & Sonder, 1990), or the result of redistribution and accumulation of radiogenic material during tectonic deformation (e.g. Huerta *et al.*, 1996; Jamieson *et al.*, 1998). A recent study by

Faccenda *et al.* (2008) attributed high metamorphic temperatures and partial melting in the Himalaya in part to the widespread occurrence of metasedimentary rocks with radiogenic heat production of 4–5  $\mu\text{W m}^{-3}$ . In our model, a layer 5 km thick with elevated radiogenic heat production of 3 or 4  $\mu\text{W m}^{-3}$  is positioned in the overthrust region just below the interface of the two crustal plates. The initial depth of the layer is constant at 35–40 km for  $x = 0$ –60 km and then decreases linearly from 35 to 0 km at  $x = 60$ –120 km. The layer is propagated upwards with exhumation and reaches the surface at the end of the simulation. The heat production below the layer drops exponentially with a characteristic length scale of 10 km; the upper plate has the default value of radiogenic heat production.

An enhanced generation of heat in the vicinity of the fault zone, as introduced in this model, may in part be provided by frictional heating and viscous heating between the two converging plates, at least early in the thrust evolution. It has been suggested by Burg & Gerya (2005) that the heat production by viscous dissipation during collisional orogeny may be on average 0.1–0.3  $\mu\text{W m}^{-3}$  in the case of rheologically strong lower crust and may even reach 1–10  $\mu\text{W m}^{-3}$  over a few millions of years of intensive deformation along localized deformation zones several kilometres thick. The heat production of 3 or 4  $\mu\text{W m}^{-3}$  within a 5 km thick layer at the fault zone in our models, therefore, may be envisioned, in part, to result from shear heating and viscous dissipation.

Figure 5(a) demonstrates the results for the two models for an erosion rate of 1 mm year<sup>-1</sup>. The  $P$ - $T$ - $t$  paths are displaced to considerably higher temperatures in comparison with the model with the standard thermal structure (Fig. 2a). The deep rocks in the absence of reaction are heated up to 720 °C for  $A_{\text{en}} = 3 \mu\text{W m}^{-3}$  and 780 °C for  $A_{\text{en}} = 4 \mu\text{W m}^{-3}$  (Fig. 5a,b; Table 3). The effect of dehydration is correspondingly increased: the drop in the peak temperatures due to reaction in the two models is above 35 and 45 °C respectively (Fig. 5g). At a given time, the temperature difference between the reacting and non-reacting rocks may reach 60 °C along their respective  $P$ - $T$ - $t$  paths ( $A_{\text{en}} = 4 \mu\text{W m}^{-3}$ , Fig. 4c). The stronger thermal effect of reactions in these models is the result of elevated dehydration due to faster rates of temperature change; the amount of expelled fluid for the rocks in the underthrust section is more than 1 wt% greater than in the reference model (Fig. 5e). As a result, chemical reactions in deep rocks

**Fig. 3.** Model results for average values of radiogenic heat production and basal heating; erosion starts at 10 Myr with the rate of 1 mm year<sup>-1</sup>. (a)  $P$ - $T$ - $t$  paths are shown with thick lines; dashed for the no reaction case ( $\Delta H = 0$ ), dotted for prograde reaction ( $\Delta H > 0$ ), solid for prograde and retrograde reaction ( $\Delta H \leq 0$ ). (b) Crustal geotherms at 0 and 15 Myr are shown with thin lines; dashed for no reaction case, solid for prograde and retrograde reaction. (c) Temperature difference at constant pressure between reacting ( $\Delta H \leq 0$ ) and non-reacting rocks. (d) Pressure difference at constant temperature between reacting ( $\Delta H \leq 0$ ) and non-reacting rocks. (e) Temporal evolution of the fraction of bound water in crustal rocks ( $\Delta H \leq 0$ ). (f) Temporal evolution of the cumulative heat of reaction ( $\Delta H \leq 0$ ). (g) The 2D distribution of the difference in peak temperatures (solid lines, °C) and the timing of thermal peak (dashed lines, Ma) between the reacting ( $\Delta H \leq 0$ ) and non-reacting model at the end of the simulation.

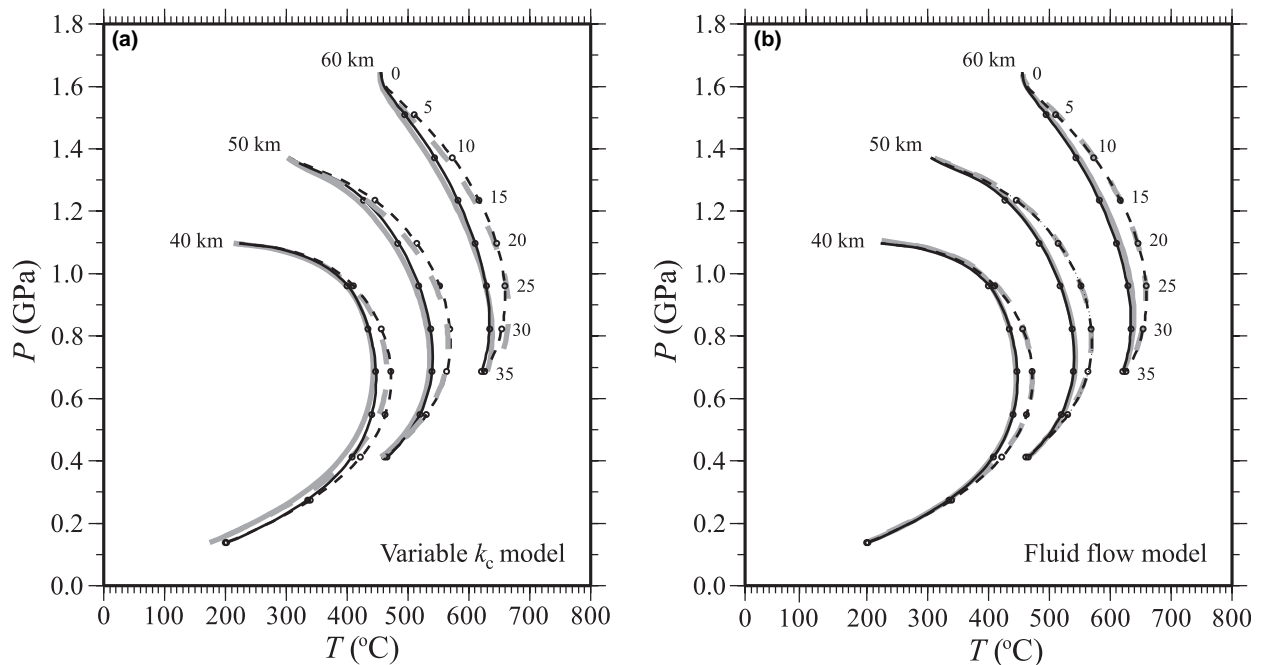


**Fig. 4.** (a) Comparison of model results for constant and temperature-dependent thermal conductivity,  $k_c$ .  $P$ - $T$ - $t$  paths are shown with thin black lines for constant  $k_c$  and with thick grey lines for temperature-dependent  $k_c$ ; dashed for no reaction case, solid for prograde and retrograde reaction. (b) The comparison of the model results with and without fluid flow.  $P$ - $T$ - $t$  paths are shown with thin black lines for the default model and with thick grey lines for model with fluid flow; dashed for no reaction case, solid for prograde and retrograde reaction.

consume at least  $100 \text{ kJ l}^{-1}$  more energy than those in the reference model (compare Figs 2f & 5f).

The above calculations demonstrate that progressive elevation of heating rates within the crust in a collisional setting will lead to acceleration of metamorphic reaction rates and the corresponding increase in the effect of reaction on the orogen thermal structure. In particular, for a rock initially at 50 km depth, the drop in the peak temperature due to dehydration reactions is about 5.3% in the reference model (from 570 to 541 °C), 5.8% in a model with  $A_{\text{en}} = 3 \mu\text{W m}^{-3}$  (from 639 to 602 °C) and 6.5% for a model with  $A_{\text{en}} = 4 \mu\text{W m}^{-3}$  (from 707 to 661 °C). It must be noted, however, that even under these conditions of more extensive dehydration due to a strong crustal heat source ( $A_{\text{en}} = 4 \mu\text{W m}^{-3}$ ), none of the rocks in the lower plate of the collisional zone become fully dehydrated, and most retain more than 1 wt% of water.

An alternative scenario is tested in which rock temperatures in the collisional zone are elevated due to a strong increase in basal heating in the overthrust region after the end of collision. Such intensive heating from below may be the result of the attenuation or removal of the mantle lithosphere through delamination or detachment, or the consequence of plutonic activity below the base of the crust (e.g. Loosveld & Etheridge, 1990; Bodorkos *et al.*, 2002). Two models are examined with basal heat flow within the overthrust region at 60 and 90  $\text{mW m}^{-2}$ , and the average

value for the basal heat flow (30  $\text{mW m}^{-2}$ ) away from the thrust. The effect of metamorphic reaction in this scenario is smaller than in the case of elevated heating rates due to radiogenic crustal sources: the drop in peak temperatures is about 30 °C for  $q_b = 60 \text{ mW m}^{-2}$  and  $\sim 35 \text{ °C}$  for  $q_b = 90 \text{ mW m}^{-2}$ . The smaller temperature drop due to reaction in this model is explained by the comparatively localized effect of the basal heat source on the thermal structure of the model orogen. The mantle heat source mostly affects the deepest crustal rocks (60–70 km), whereas large volumes of shallower rocks undergo only moderate heating (e.g. compare the peak temperatures for the crustal radiogenic source model and elevated basal heat flow model at 50 and 60 km, Table 3).

#### The effect of lithology

Finally, we test the thermal effects of metamorphic reactions that occur in a single layer containing both metapelitic and metacarbonate rocks. The layer has a thickness of 10 km, a lateral extent of 30 km, and is located at 35–45, 45–55 or 55–65 km depths in different models (Table 3). The fraction of metacarbonate rocks within the layer is 20, 50 or 80%, with metapelitic rocks comprising the rest of the layer mass. The dehydration reactions in metapelites proceed continuously in the temperature interval 200–750 °C, whereas decarbonation reactions in the metacarbonate fraction occur in discrete episodes at

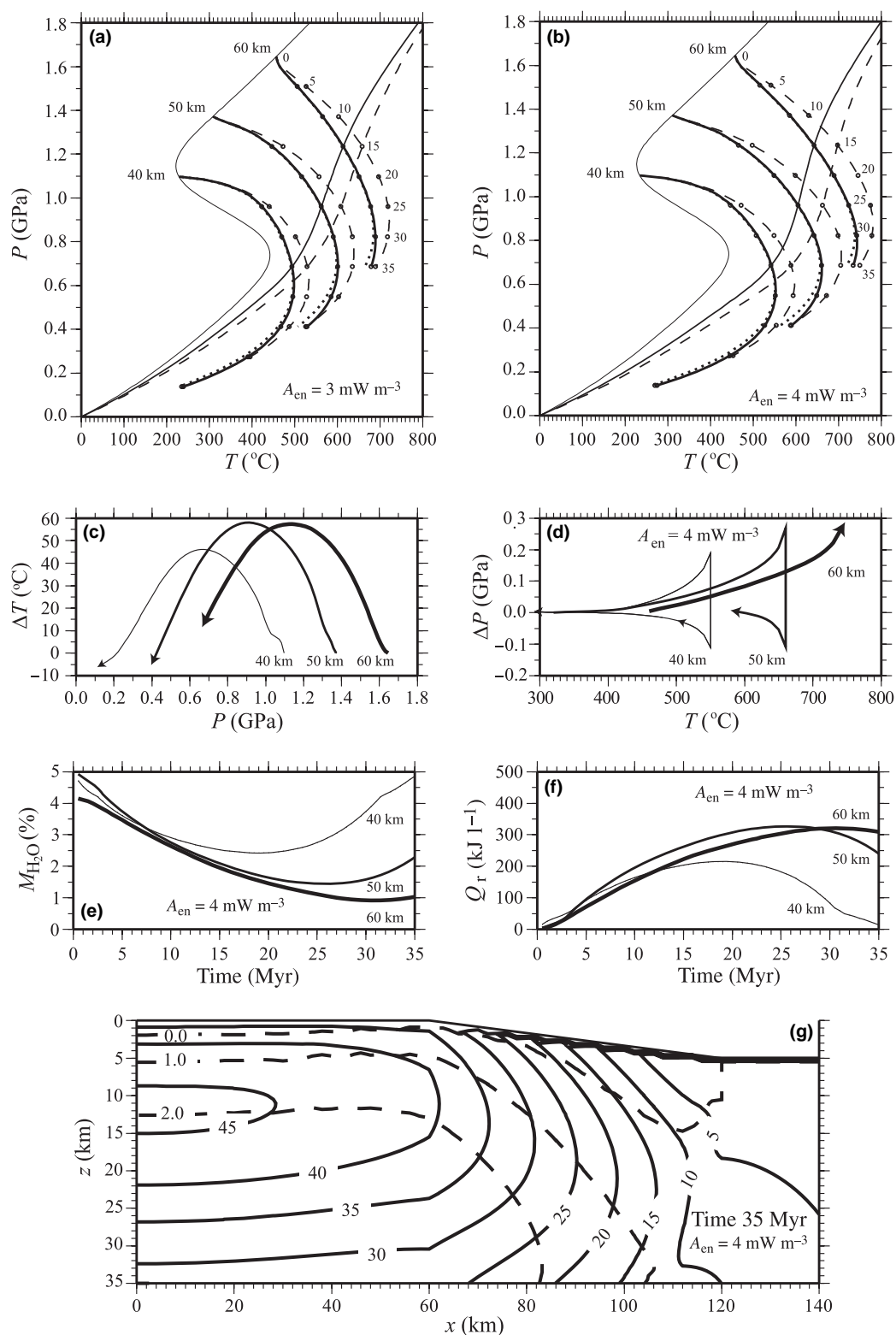
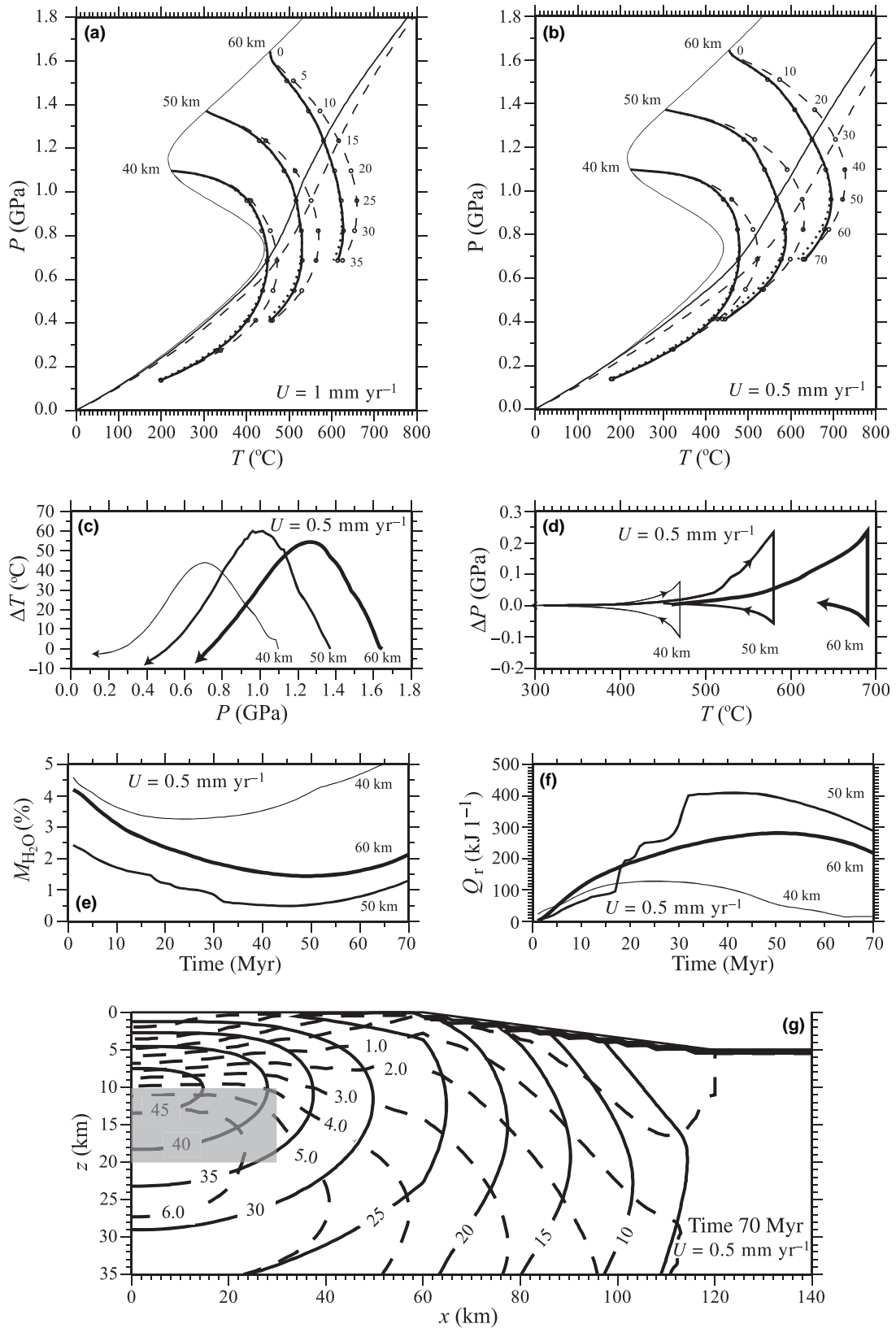


**Fig. 5.** Model results for the thermal structure with a layer enriched in radiogenic elements, initial layer depth 35–30 km. Notation as in Fig. 2. (a) Heat production in the enriched layer is  $3 \mu\text{W m}^{-3}$ . (b)–(f) Heat production in the enriched layer is  $4 \mu\text{W m}^{-3}$ . (g) The 2D distribution of the difference in peak temperatures (solid lines,  $^{\circ}\text{C}$ ) and the timing of the thermal peak (dashed lines, Ma) between the reacting ( $\Delta H \leq 0$ ) and non-reacting model at the end of the simulation; heat production in the enriched layer is  $4 \mu\text{W m}^{-3}$ .



500, 530, 545 and 570 °C on the heating path of a reacting rock.

The results for two models that include a layer composed of 50 wt% metapelite and 50 wt% metacarbonate at 45–55 km depth are shown in Fig. 6(a–g). The models have a standard thermal structure and erosion rates of 1 or 0.5 mm year<sup>-1</sup>. The *P–T–t* paths for the faster erosion rate (Fig. 6a) are not much different from those in our default model with the same erosion (Fig. 2a). The maximum drop in peak temperatures is only slightly above 35 °C (in the absence of metacarbonate rocks the drop is 25–29 °C; Table 3). The decarbonation reaction leads to temperature buffering within the layer at 500 and 530 °C between 10 and 20 Myr of the exhumation history. No further decarbonation episodes occur in this relatively cold model as temperature within the layer never reaches the equilibrium condition for transition to the amphibole zone (545 °C).

At lower erosion rates, however, the thermal effect of decarbonation reaction is much stronger; the longer exhumation history leads to higher rock temperatures and a correspondingly greater amount of energy available for chemical work (Fig. 6b). The intensive metamorphism within the metacarbonate-bearing layer leads to an ~45 °C drop in metamorphic peak temperatures and more than a 6 Myr delay in peak temperature attainment (Fig. 6g). At the time of intensive decarbonation (15–35 Myr) the temperature difference between reacting and non-reacting rock can exceed 60 °C (Fig. 6b). All four episodes of decarbonation occur within the metacarbonate-bearing layer; the three transitions that consume large amounts of heat (to the biotite zone, amphibolite zone and diopside zone) are clearly marked by steep gradients in the  $Q_r$  plot (Fig. 6f). The total amount of heat consumed by reactions within the layer is about 410 kJ l<sup>-1</sup> (Fig. 6f), whereas full dehydration and decarbonation of a layer with this composition would require about 460 kJ l<sup>-1</sup> of energy. Note that the temporal changes in the mass of chemically bound water,  $M_{H_2O}$ , reflect only the progress of dehydration reactions in metapelitic rocks (Fig. 6e). For rocks within the metacarbonate-bearing layer (initial depth 50 km), inflections in the  $M_{H_2O}$  graph are produced by the changes in the rates of dehydration reaction in response to the thermal buffering caused by decarbonation.

Because the amount of energy entering the metacarbonate-bearing layer is crucial in driving both dehydration and decarbonation reactions, not only erosion rates but also the positioning of the layer will

determine the thermal effect produced by metamorphism. In particular, a shallow metacarbonate-bearing layer in a setting with fast exhumation rates in the absence of additional heat sources may never attain temperatures that will trigger decarbonation reactions. On the contrary, if the metacarbonate-bearing layer is buried below 50 km, it will undergo intensive dehydration and decarbonation reactions that may decrease the peak metamorphic temperatures by more than 50 °C (see Table 3 for details).

A series of simulations exploring the effects of different metacarbonate–metapelite fractions in the metacarbonate-bearing layer is summarized in Table 3. Decarbonation reactions generally have larger enthalpies per mole of fluid released than dehydration reactions and therefore have more capacity to control temperature within the reacting rock. Predictably then, a larger proportion of metacarbonate rocks within the layer increases the thermal effect of reaction and further reduces the metamorphic peak temperatures.

The last set of models explores the thermal effect of reaction in a metacarbonate-bearing layer at 45–55 km depth with an additional crustal heat source below the fault zone (heat production  $A_{cn} = 4 \mu\text{W m}^{-3}$ , Table 3). Despite relatively fast erosion of 1 mm year<sup>-1</sup>, the considerable amount of heat produced in the crust drives very intensive devolatilization in the lower part of the crust and especially within the metacarbonate-bearing layer (Fig. 7a–f). The drop in the peak temperature in the vicinity of the layer is 60–65 °C (Fig. 7f), the temperature difference between reacting and non-reacting rock at 1 GPa is almost 100 °C (Fig. 7b). The pressure difference between the reacting and non-reacting *P–T–t* paths is also increased to above 0.3 GPa at peak metamorphic conditions (Fig. 7c). By 20 Myr, metamorphic reactions within the rocks initially at 50 km depth consumed about 430 kJ l<sup>-1</sup> out of the total 460 kJ l<sup>-1</sup> that are required for full devolatilization of metacarbonate and metapelitic rocks in the layer. As in the previous models, increasing the fraction of reacting metacarbonate rocks within the layer will further elevate the thermal effect of metamorphic reactions; if the proportion of metacarbonate rocks is 80%, peak temperatures will decrease by an additional 10–15 °C (Table 3).

## DISCUSSION AND CONCLUSIONS

The results of our simulations for the ‘standard’ overthrust model with average values of crustal radiogenic heating and basal heat flow demonstrate that dehy-

**Fig. 6.** Results for the model with a metacarbonate-bearing layer 30 km wide at an initial depth 45–55 km; the fraction of metacarbonate rock is 50%. Notation as in Fig. 2. (a) Erosion rate 1 mm year<sup>-1</sup>. (b)–(f) Erosion rate 0.5 mm year<sup>-1</sup>. In part (e), a rock initially at 50 km depth is within the metacarbonate-bearing layer; the mass of bound water shown for this rock is from its metapelitic fraction. (g) The 2D distribution of the difference in peak temperatures (solid lines, °C) and the timing of the thermal peak (dashed lines, Ma) between the reacting ( $\Delta H \leq 0$ ) and non-reacting model at the end of the simulation; erosion rate 0.5 mm year<sup>-1</sup>. The position of the metacarbonate-bearing layer at the end of the simulation is shown with a grey rectangle.

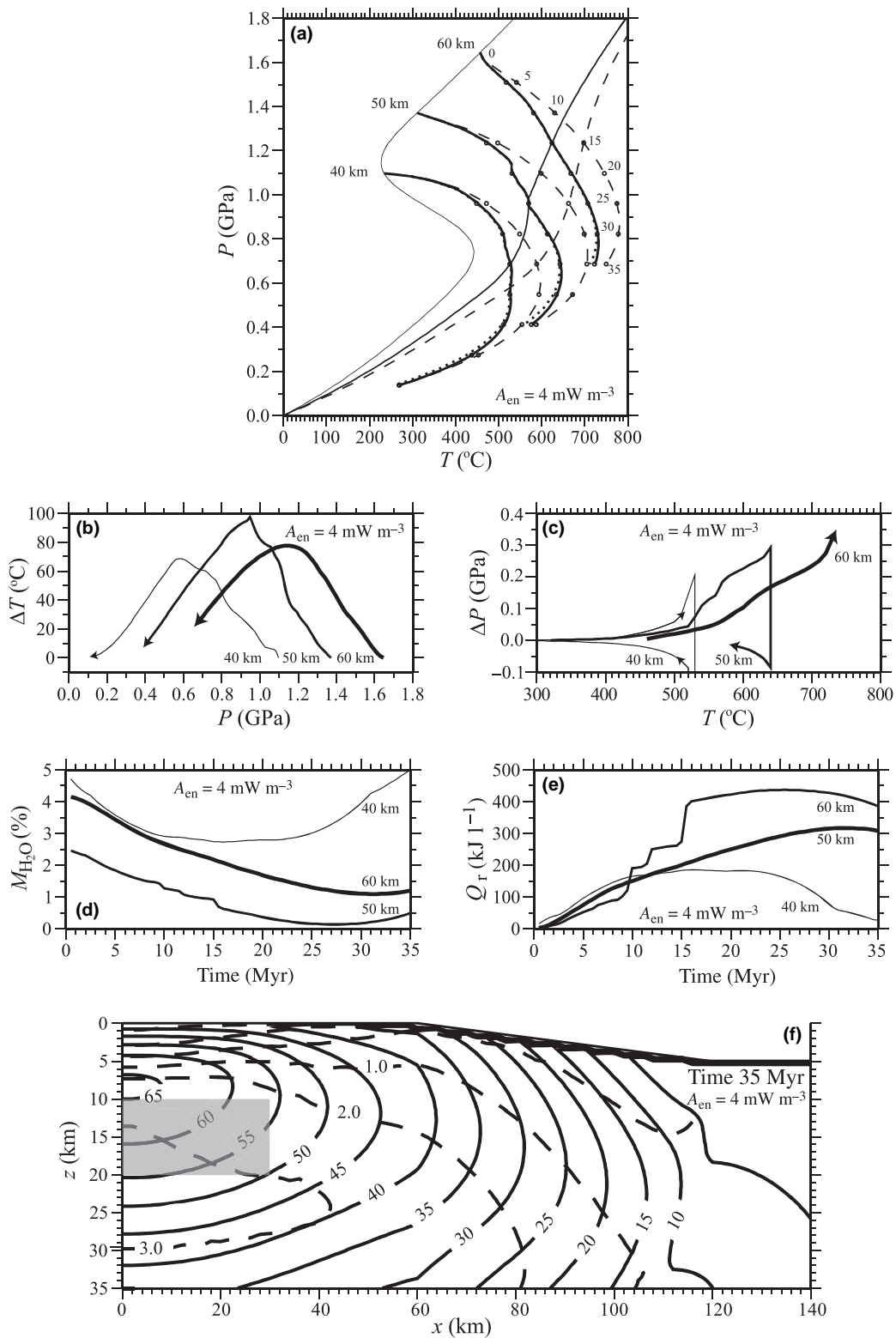


**Fig. 7.** Results for the model with a metacarbonate-bearing layer 30 km wide at the initial depth 45–55 km with the fraction of metacarbonate rock 50%; and a layer enriched in radiogenic elements, with heat production of  $4 \mu\text{W m}^{-3}$  and initial depth 35–30 km. Erosion rate  $\text{mm year}^{-1}$ . Notation as in Fig. 3. In part (d), a rock initially at 50 km depth is within the metacarbonate-bearing layer; the mass of bound water shown for this rock is from its metapelite fraction. (f) The 2D distribution of the difference in peak temperatures (solid lines,  $^{\circ}\text{C}$ ) and the timing of the thermal peak (dashed lines, Ma) between the reacting ( $\Delta H \leq 0$ ) and non-reacting model at the end of the simulation. The position of the metacarbonate-bearing layer at the end of the simulation is shown with a grey rectangle.

dration reactions which occur during prograde heating of crustal rocks of pelitic composition will reduce the peak metamorphic temperatures by 25–40 °C (Figs 2 & 3, Table 3). Relative to the non-reacting case,  $P$ – $T$ – $t$  paths are changed such that peak temperature attainment for rocks in the underthrust region is retarded by several Myr (>2 Myr at erosion  $U = 1 \text{ mm year}^{-1}$  and >4 Myr for  $U = 0.5 \text{ mm year}^{-1}$ ). Moreover, the pressures at which peak temperatures are attained are about 0.25 GPa less when the prograde reactions are accounted for. The effect of hydration reaction in our models is relatively small (Table 3). The peak metamorphic temperatures in models that include retrograde reactions are generally 2–5 °C higher than in the models without retrograde metamorphism.

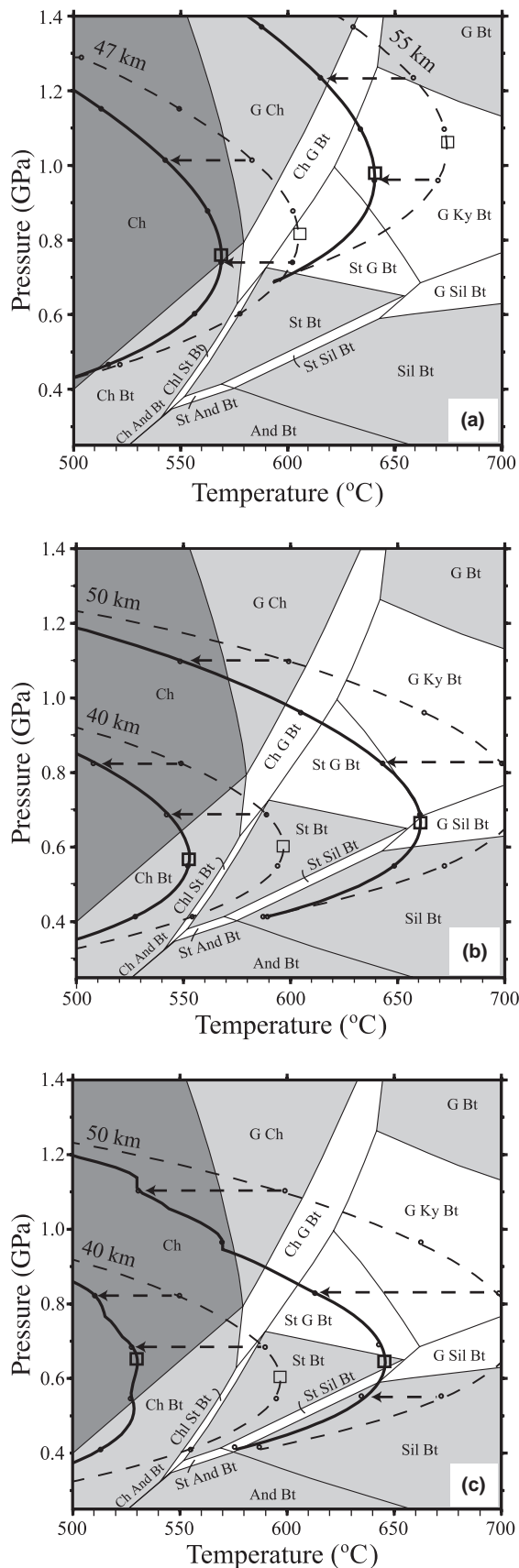
The thermal effect of dehydration reactions in our simulations is slightly smaller than the 50 °C suggested by Peacock (1989); the difference is probably due to the neglect of exhumation in his model. Despite some difference in parameters between our work and that of Connolly & Thompson (1989) (e.g. exhumation rates and the rates of reaction), the results for peak temperatures in both our study and theirs are in general agreement for the ‘standard’ overthrust model. Connolly & Thompson (1989) stated that the drop in peak temperatures due to reaction is below 40 °C, whereas their figures show about 20 °C temperature difference between reacting and non-reacting examples. The relatively modest decrease in peak temperatures of 25–40 °C in our model, however, is the direct consequence of low heating rates characteristic of the collisional overthrust setting with average values of crustal and mantle heat sources. As dehydration reactions in metapelitic rocks are mainly controlled by the rates of temperature change in the system, low heating rates lead to slow reaction and correspondingly low values of heat consumption by chemical work. Indeed, our calculations demonstrate that only about half of the water supply available for dehydration is processed during the evolution of the ‘standard’ thrust model. Nonetheless, even for these examples involving fairly limited devolatilization, it is emphasized that the timing of peak temperature attainment is significantly delayed by 2–4 Myr, and that the pressure of peak temperature attainment is reduced by ~2.5 GPa relative to models which ignore reaction enthalpy.

It must be noted here that the temperature differences of 30–40 °C, although relatively small in comparison with the total temperature variation in the overthrust model, are non-trivial from the point of view of metamorphic petrology and may lead to considerable changes in mineral assemblages. On Fig. 8(a), the  $P$ – $T$ – $t$  paths are plotted for our default model with delayed erosion on a pseudosection for a representative metapelitic composition from Powell *et al.* (1998). Depending on their initial depth, the mineralogical pathways of the exhumed rocks may be considerably affected by metamorphic dehydration reactions. In particular, a rock exhumed from a depth

of 47 km is predicted to attain peak conditions in the amphibolite facies (staurolite zone) if the enthalpy effects of reaction are not considered. However, if the enthalpy effects of moderate dehydration (with ~2.5 wt% loss of fluid) are taken into account, the peak assemblage is grossly different, corresponding to the chlorite–biotite zone boundary in the greenschist facies.

The field study by Ferry (1983), which evaluated the amount of heat consumed by metamorphic reactions in impure carbonate rocks in south-central Maine, may be regarded as a benchmark case for numerical modelling of the extent of reaction in the rock with mixed metacarbonate–metapelitic composition. The field data suggest that more than 400 kJ l<sup>-1</sup> of energy was consumed by reaction within metacarbonate rocks. Our calculations show that the model metacarbonate-bearing layer at mid-crustal depths in the overthrust setting with the average thermal structure and an erosion rate of 1 mm year<sup>-1</sup> will consume only about 200 kJ l<sup>-1</sup> of heat due to the insufficient amount of energy for driving the decarbonation reaction (Fig. 6a). In this case, as in the case with average metapelitic rock composition, our default model does not provide enough energy for driving intensive devolatilization. The progress of metamorphic reactions and their effect on the thermal structure of the overthrust model, therefore, are mainly controlled by the amount of energy available in the system for driving the devolatilization. The limited amount of metamorphism within the ‘standard’ thrust model is thus directly linked to the bigger problem of ‘missing heat’ as stated by Jamieson *et al.* (1998) and others. The nappe stacking of continental crust with the average thermal structure and realistic erosion rates is unlikely to provide enough heat to produce Barrovian  $P$ – $T$  conditions, and by the same token, to drive extensive metamorphic devolatilization.

Our simulations of overthrust evolution with additional heat sources in the crust and the mantle demonstrate that elevated rates of dehydration reactions in metapelites may reduce the peak metamorphic temperatures in the overthrust zone by more than 45 °C. This decrease in temperature translates into considerable changes in mineralogical pathways of metamorphosed rocks (Fig. 8b). In particular, a rock exhumed from the depth of 40 km is predicted to have a greenschist facies peak mineral assemblage (biotite zone) if the enthalpy of reaction is taken into account, and an amphibolite facies assemblage (staurolite zone) if the reaction enthalpy is neglected. A deeper rock, exhumed from 50 km depth, will have a peak assemblage corresponding to the sillimanite zone of the amphibolite facies in both cases. However, if no thermal effects of reaction are considered, the rock is predicted to pass through the kyanite stability field; it is likely to preserve kyanite as inclusions in garnet porphyroblasts and other textural features. With thermal effects of reaction taken into account, the rock will enter the sillimanite zone



through the staurolite stability field. Even in this model with elevated heating rates, however, the amount of energy consumed by reaction in our simulations is only 70–80% of the amount of heat that would be required for the full dehydration of crustal rocks with average pelitic composition. By the end of the prograde history of the thrust, the deep rocks retain from 0.5 to 2.5 wt% of the chemically bound water available for dehydration.

The inclusion of a single layer 10 km thick with mixed metacarbonate–metapelitic composition in a model with elevated heating rates leads to dramatic changes in the  $P$ – $T$ – $t$  paths of the deep rocks, mainly due to the thermal controls exerted by decarbonation reactions (Figs 7 & 8c). These  $P$ – $T$ – $t$  paths may to some extent reflect the history of metacarbonate rocks studied by Ferry (1992, 1994). Such reaction sequences, however, appear to be common in Barrovian terranes (e.g. Ague, 2003). The peak temperatures in this model are reduced by more than 60 °C, and the pressures at which the peak temperatures are attained decrease by 0.3 GPa, corresponding to a difference in depth of more than 10 km. The mineralogical pathways of the exhumed metapelitic rocks are greatly affected by the thermal effects of reactions (Fig. 8c). A metapelitic rock exhumed from a depth of 40 km is predicted to attain peak conditions in the chlorite zone of the greenschist facies if the enthalpy of reaction is taken into account, and in the staurolite zone of the amphibolite facies if the reaction enthalpy is ignored. For a rock initially at 50 km depth, the thermal effects of reaction will change the peak assemblage from that in the sillimanite field of the amphibolite facies, to the staurolite stability field. The effect is even stronger when the fraction of metacarbonate rocks in the layer is increased from 50% to 80% (Table 3).

Numerical models reported in this work admittedly present a simplified picture of the thermal evolution of collisional orogens. We consciously ignore many processes that occur during orogeny, such as crustal deformation and faulting, the production and movement of magmas, and temporal variability in exhumation and erosion rates. All of these processes are likely to affect the rates of heating and cooling of crustal rocks, the shapes of the  $P$ – $T$ – $t$  paths and

**Fig. 8.** Model  $P$ – $T$ – $t$  paths plotted on a representative pseudo-section for metapelitic rocks from Powell *et al.* (1998). (a) Model with the average value of crustal and mantle heating and delayed erosion (1 mm year<sup>-1</sup> after 10 Myr). Dashed lines are for the case with no reaction, solid lines for prograde and retrograde reaction. Circles denote time increments of 5 Myr; squares indicate the peak metamorphic conditions. (b) Model with a layer enriched in radiogenic elements, heat production within the layer is 4  $\mu\text{W m}^{-3}$ . Notation as in part (a). (c) Model with a layer enriched in radiogenic elements (heat production 4  $\mu\text{W m}^{-3}$ ) and a metacarbonate-bearing layer 30 km wide at an initial depth 45–55 km containing 50% metacarbonate rock. Notation as in part (a).

consequently, the rates and thermal effects of metamorphic reactions. Nonetheless, as evident from the petrological observations of reaction progress, fluid flow and hydrofracturing in metamorphic rocks (e.g. Ferry, 1983; Ague, 1994), the burial and consequent exhumation of metasedimentary rocks inevitably leads to their devolatilization and the accompanying thermal effects. In composing the inventory of the heat sources for Barrovian metamorphism during orogenic collision the heat sink provided by metamorphic devolatilization reactions thus should not be neglected. Elevated heating rates required for the production of the Barrovian metamorphic conditions are likely to result in intensive devolatilization reactions and noticeable heat consumption. In particular, viscous dissipation during mechanical deformation in the thrust fault, which potentially may lead to temperature increases of 25–200 °C over short time scales of 5–10 Myr (Burg & Gerya, 2005), is likely to trigger strong devolatilization in the deformed rock with the subsequent consumption of a large portion of viscous heat.

The lithology of rocks composing the collision zone may also have important consequences for its temperature evolution if metamorphic reactions are included in the thermal budget calculations. Petrological data suggest that as much as 25% of crustal sedimentary rock settings is composed of limestone and dolomite. As indicated by our results, even a single mid-crustal layer 10 km thick containing 20–50% metacarbonate rock may produce a considerable drop in peak temperatures if enough heat is provided for intensive decarbonation. Consideration of metamorphic reactions in collisional orogens containing protolith layers of carbonate composition may therefore present an additional challenge for the thermomechanical modelling of orogenic  $P$ – $T$  evolution. The problem of ‘missing heat’ in numerical models of Barrovian metamorphic terranes may thus be amplified if devolatilization reactions are taken into account. Further investigations of the thermal effects of metamorphism in specific geological localities should assess actual devolatilization and solid–solid reaction sequences and their enthalpies in a wide range of rock types and compositions.

## ACKNOWLEDGEMENTS

We thank R. Bousquet and S. Chakraborty for discussions, and T. Gerya and D. Pattison for their constructive reviews. The support of the National Science Foundation Directorate for Geosciences (NSF EAR-0509934) is gratefully acknowledged.

## REFERENCES

Ague, J.J., 1994. Mass transfer during Barrovian metamorphism of pelites, south-central Connecticut: II. Channelized fluid flow and the growth of staurolite and kyanite. *American Journal of Science*, **294**, 1061–1134.

- Ague, J.J., 1998. Simple models of coupled fluid infiltration and redox reactions in the crust. *Contributions to Mineralogy and Petrology*, **132**, 180–197.
- Ague, J.J., 2000. Release of CO<sub>2</sub> from carbonate rocks during regional metamorphism of lithologically heterogeneous crust. *Geology*, **28**, 1123–1126.
- Ague, J.J., 2003. Fluid infiltration and transport of major, minor, and trace elements during regional metamorphism of carbonate rocks, Wepawaug Schist, Connecticut, USA. *American Journal of Science*, **303**, 753–816.
- Ague, J.J. & Baxter, E.F., 2007. Brief thermal pulses during mountain building recorded by Sr diffusion in apatite and multicomponent in garnet. *Earth and Planetary Science Letters*, **261**, 500–516.
- Ague, J.J., Park, J. & Rye, D.M., 1998. Regional metamorphic dehydration and seismic hazard. *Geophysical Research Letters*, **25**, 4221–4224.
- Anderson, R.N., Delong, S.E. & Miyashiro, A., 1976. Geophysical and geochemical constraints at converging plate boundaries – part I: dehydration in the downgoing slab. *Geophysical Journal of the Royal Astronomical Society*, **44**, 333–357.
- Anderson, R.N., Delong, S.E. & Schwarz, W.M., 1978. Thermal model for subduction with dehydration in the downgoing slab. *Journal of Geology*, **86**, 731–739.
- Barr, T.D., Dahlen, F.A. & McPhail, D.C., 1991. Brittle frictional mountain building. 3. Low-grade metamorphism. *Journal of Geophysical Research*, **96**, 10319–10338.
- Baxter, E.F., Ague, J.J. & DePaolo, D.J., 2002. Prograde temperature–time evolution in the Barrovian type-locality constrained by Sm/Nd garnet ages from Glen Clova, Scotland. *Journal of Geologic Society of London*, **159**, 71–82.
- Berman, R.G., 1988. Internally-consistent thermodynamic data for minerals in the system Na<sub>2</sub>O–K<sub>2</sub>O–CaO–MgO–FeO–Fe<sub>2</sub>O<sub>3</sub>–Al<sub>2</sub>O<sub>3</sub>–SiO<sub>2</sub>–TiO<sub>2</sub>–H<sub>2</sub>O–CO<sub>2</sub>. *Journal of Petrology*, **29**, 445–522.
- Berman, R.G., 1991. Thermobarometry using multi-equilibrium calculations: a new technique, with petrological applications. *Canadian Mineralogist*, **29**, 833–855.
- Bird, P., 1978. Initiation of intracontinental subduction in the Himalaya. *Journal of Geophysical Research*, **83**, 4975–4987.
- Bird, P., Toksoz, M.N. & Sleep, N.H., 1975. Thermal and mechanical models of continent–continent convergence zones. *Journal of Geophysical Research*, **80**, 4405–4416.
- Bodorkos, S., Sandiford, M., Oliver, N.H.S. & Cawood, P.A., 2002. High- $T$ , low- $P$  in the Palaeoproterozoic Halls Creek Orogen, northern Australia: the middle crustal response to a mantle-related transient thermal pulse. *Journal of Metamorphic Geology*, **20**, 217–237.
- Burg, J.-P. & Gerya, T.V., 2005. The role of viscous heating in Barrovian metamorphism of collisional orogens: thermomechanical models and application to the Lepontine Dome in the Central Alps. *Journal of Metamorphic Geology*, **23**, 75–95.
- Cermak, V., 1993. Lithospheric thermal regimes in Europe. *Physics of the Earth and Planetary Interiors*, **79**, 179–193.
- Chamberlain, C.P. & Rumble, D., 1989. The influence of fluids on the thermal history of a metamorphic terrain: New Hampshire, USA. In: *Evolution of Metamorphic Belts* (eds (Daly, J.S., Cliff, R.A. & Yardley, B.W.D.)), Geological Society Special Publications, **43**, 203–213.
- Chamberlain, C.P. & Sonder, L.J., 1990. Heat-producing elements and the thermal and baric patterns of metamorphic belts. *Science*, **250**, 763–769.
- Connolly, J.A.D. & Thompson, A.B., 1989. Fluid and enthalpy production during regional metamorphism. *Contributions to Mineralogy and Petrology*, **102**, 347–366.
- De Yoreo, J.J., Lux, D.R. & Guldotti, C.V., 1991. Thermal modeling in low-pressure/high-temperature metamorphic belts. *Tectonophysics*, **188**, 209–238.

- Doll, C.G., Cady, W.M., Thompson, J.B.J. & Billings, M.B., 1961. Centennial geologic map of Vermont: Montpelier. *Vermont Geological Survey, scale 1:250 000*.
- Engi, M., Berer, A. & Rosselle, G.T., 2001. Role of the tectonic accretion channel in collisional orogeny. *Geology*, **29**, 1143–1146.
- England, P.C. & Thompson, A.B., 1984. Pressure–temperature–time paths of regional metamorphism. I. Heat transfer during the evolution of regions of thickened continental crust. *Journal of Petrology*, **25**, 894–928.
- Faccenda, M., Gerya, T.V. & Chakraborty, S., 2008. Styles of post-subduction collisional orogeny: Influence of convergence velocity, crustal rheology and radiogenic heat production. *Lithos*, **103**, 257–287.
- Ferry, J.M., 1980. A case study of the amount and distribution of heat and fluid during metamorphism. *Contributions to Mineralogy and Petrology*, **71**, 373–385.
- Ferry, J.M., 1983. On the control of temperature, fluid composition, and reaction progress during metamorphism. *American Journal of Science*, **283**, 201–232.
- Ferry, J.M., 1992. Regional metamorphism of the Waits River Formation, eastern Vermont: delineation of a new type of giant metamorphic hydrothermal system. *Journal of Petrology*, **33**, 45–94.
- Ferry, J.M., 1994. Overview of the petrologic record of fluid flow during regional metamorphism in Northern New England. *American Journal of Science*, **294**, 905–988.
- Ferry, J.M. & Spear, F.S., 1978. Experimental calibration of the partitioning of Fe and Mg between biotite and garnet. *Contributions to Mineralogy and Petrology*, **66**, 113–117.
- Gerya, T.V., Perchuk, L.L., Maresch, W.V., Willner, A.P., Van Reenen, D.D. & Smit, C.A., 2002. Thermal regime and gravitational instability of multi-layered continental crust: implications for the buoyant exhumation of high-grade metamorphic rocks. *European Journal of Mineralogy*, **14**, 687–699.
- Goffé, B., Bousquet, R., Henry, P. & LePichon, X., 2003. Effect of the chemical composition of the crust on the metamorphic evolution of orogenic wedges. *Journal of Metamorphic Geology*, **21**, 123–141.
- Haack, U.K. & Zimmermann, H.D., 1996. Retrograde mineral reactions: a heat source in the continental crust? *Geologische Rundschau*, **85**, 130–137.
- Hanson, R.B., 1997. Hydrodynamics of regional metamorphism due to continental collision. *Economic Geology*, **92**, 880–891.
- Hanson, R.B. & Barton, M.D., 1989. Thermal development of low-pressure metamorphic belts: Results from two-dimensional numerical models. *Journal of Geophysical Research*, **94**, 10363–10377.
- Holland, T.J.P. & Powell, R., 1991. A Compensated–Redlich–Kwong (CORK) equation for volumes and fugacities of CO<sub>2</sub> and H<sub>2</sub>O in the range 1 bar to 50 kbar and 100–1600 °C. *Contributions to Mineralogy and Petrology*, **109**, 265–273.
- Holland, T.J.P. & Powell, R., 1998. An internally consistent thermodynamic data set for phases of petrological interest. *Journal of Metamorphic Geology*, **16**, 309–343.
- Huerta, A.D., Royden, L.H. & Hodges, K.V., 1996. The interdependence of deformational and thermal processes in mountain belts. *Science*, **273**, 637–639.
- Huerta, A.D., Royden, L.H. & Hodges, K.V., 1998. The thermal structure of collisional orogens as a response to accretion, erosion and radiogenic heating. *Journal of Geophysical Research*, **103**, 15287–15302.
- Jamieson, R.A., Beaumont, C., Fullsack, P. & Lee, B., 1998. Barrovian regional metamorphism: where's the heat? In: *What Drives Metamorphism and Metamorphic Reactions?* (eds Treolar, P.J. & O'Brien, P.J.), *Geological Society, London, Special Publications*, **138**, 23–51.
- Jamieson, R.A., Beaumont, C., Nguyen, M.H. & Lee, B., 2002. Interaction of metamorphism, deformation and exhumation in large convergent orogens. *Journal of Metamorphic Geology*, **20**, 9–24.
- Jaupart, C. & Mareschal, J.-C., 2003. Constraints on crustal heat production from heat flow data. In: ???? (eds Holland, H. & Turekian, K.K.), *Treatise on Geochemistry*, **3**, 65–84.
- Loosveld, R.J.H. & Etheridge, M.A., 1990. A model for low-pressure facies metamorphism during crustal thickening. *Journal of Metamorphic Geology*, **8**, 257–267.
- Luttge, A., Bolton, E.W. & Rye, D.M., 2004. A kinetic model of metamorphism: an application to siliceous Dolomites. *Contributions to Mineralogy and Petrology*, **146**, 546–565.
- Lux, D.R., De Yoreo, J.J., Guldotti, C.V. & Decker, E.R., 1986. Role of plutonism in low-pressure metamorphic belt formation. *Nature*, **323**, 794–797.
- Lyubetskaya, T. & Ague, J.J., 2009. Modeling the magnitudes and directions of regional metamorphic fluid flow in collisional orogens. *Journal of Petrology*, **50**, 1505–1531.
- Manning, C.E. & Ingebritsen, S.E., 1999. Permeability of the continental crust: implications of geothermal data and metamorphic systems. *Reviews of Geophysics*, **37**, 127–150.
- Molnar, P. & England, P.C., 1990. Temperatures, heat flux, and frictional stress near major thrust faults. *Journal of Geophysical Research*, **95**, 4833–4856.
- Pattison, D.R.M., 2006. The fate of graphite in prograde metamorphism of pelites: an example from the Ballachulish aureole, Scotland. *Lithos*, **88**, 85–99.
- Pattison, D.R.M. & Tinkham, D.K., 2009. Interplay between equilibrium and kinetics in prograde metamorphism of pelites: an example from the Nelson aureole, British Columbia. *Journal of Metamorphic Geology*, **27**, 249–279.
- Peacock, S.M., 1987. Thermal effects of metamorphic fluids in subduction zones. *Geology*, **15**, 1057–1060.
- Peacock, S.M., 1989. Numerical constraints on rates of metamorphism, fluid production, and fluid flux during regional metamorphism. *Geological Society of America Bulletin*, **101**, 476–485.
- Peacock, S.M., 1990. Numerical simulations of metamorphic pressure–temperature–time paths and fluid production in subducting slabs. *Tectonics*, **9**, 1197–1211.
- Peacock, S.M., 1991. Numerical simulation of subduction zone metamorphic pressure–temperature–time paths: constraints on fluid production and arc magmatism. *Philosophical Transactions of the Royal Society of London*, **335**, 341–353.
- Powell, R., Holland, T.J.P. & Worley, B., 1998. Calculating phase diagrams involving solid solutions via non-linear equations, with examples using THERMOCALC. *Journal of Metamorphic Geology*, **16**, 577–588.
- Richardson, S.W. & England, P.C., 1979. Metamorphic consequences of crustal eclogite production in overthrust orogenic zones. *Earth Planetary Science Letters*, **2**, 183–190.
- Ridley, J., 1986. Modelling of the relations between reaction enthalpy and the buffering of reaction progress in metamorphism. *Mineralogical Magazine*, **50**, 375–384.
- Royden, L.H., 1993. The steady state thermal structure of eroding orogenic belts and accretionary prisms. *Journal of Geophysical Research*, **98**, 4487–4507.
- Rudnick, R.L., McDonough, W.F. & O'Connell, R.J., 1998. Thermal structure, thickness and composition of continental lithosphere. *Chemical Geology*, **145**, 395–411.
- Slater, J.G., Parsons, B. & Jaupart, C., 1981. Oceans and continents: similarities and differences in the mechanisms of heat loss. *Journal of Geophysical Research*, **86**, 11535–11552.
- Shi, Y. & Wang, C.-Y., 1987. Two-dimensional modeling of the P–T–t paths of regional metamorphism in simple overthrust terrains. *Geology*, **15**, 1048–1051.
- Turcotte, D.L. & Schubert, G., 2002. *Geodynamics: Applications of Continuum Physics to Geological Problems*. John Wiley & Sons, New York, 456 pp.

- Walder, J. & Nur, A., 1984. Porosity reduction and crustal pore pressure development. *Journal of Geophysical Research*, **89**, 11539–11548.
- Walther, J.V. & Orville, P.M., 1982. Volatile production and transport during metamorphism. *Contributions to Mineralogy and Petrology*, **79**, 252–257.
- Wilbur, D.E. & Ague, J.J., 2006. Chemical disequilibrium during garnet growth: Monte Carlo simulations of natural crystal morphologies. *Geology*, **34**, 689–692.

## APPENDIX

### Model

The geometry of the 2D model is presented on Fig. 1. The initial thermal structure is calculated based on a steady-state crustal geotherm (Turcotte & Schubert, 2002):

$$T = T_s + \frac{q_b z}{k_c} + \frac{A z_A^2}{k_c} (1 - e^{-z/z_A}).$$

The right boundary is maintained at the steady-state temperature distribution over the entire simulation time. The left boundary is symmetrical, and does not transfer heat in the horizontal dimension; the surface has a constant temperature  $T_s = 0$  °C.

Thermal conductivity is fixed at  $k_c = 2.25 \text{ W m}^{-1} \text{ K}^{-1}$  except when otherwise stated (see Table 3 for the list of simulations). In case of variable conductivity, the relationship between  $k_c$  and temperature is for dioritic composition within the crust:  $k_c = 0.91 + 641/(T + 77)$ ; and ultramafic composition in the mantle:  $k_c = 0.73 + 1293/(T + 77)$  as suggested by Gerya *et al.* (2002).

The model exhumation is at a constant rate within the flat section of topography, and is slope-dependent in the tapering section; no exhumation occurs away from the topographic elevation ( $x > 120$  km). The model topography is steady-state and is not levelled with erosion. The maximum exhumation rates of 0.5 and 1 mm year<sup>-1</sup> are tested. Simulations are stopped when the entire thickness of the emplaced crustal sheet (35 km) is removed with exhumation. The crust–mantle boundary within the thrust section is therefore transferred from the initial depth of 70 to 35 km at the end of the simulation (Fig. 1).

The model for fluid flow in the overthrust setting is presented in Lyubetskaya & Ague (2009). In addition to the energy equation, the model solves for mass conservation and momentum conservation equations for compressible fluid (see Table 1 for the list of variables):

$$\nabla \cdot \mathbf{u} = \frac{X_f \rho_m}{\Delta T} \frac{\partial T}{\partial t} - \frac{\partial(\phi \rho)}{\partial t},$$

$$\mathbf{u} = -\frac{\rho \bar{k}_\phi}{\mu_f} (\nabla P - \rho \mathbf{g}).$$

This model is used to test the effects of the fluid flow in an overthrust model with average metapelitic rock composition. For simplicity, it is assumed that metamorphic fluids are composed solely of water. The densities of water in a wide range of pressures and temperatures are calculated using the Compensated–Redlich–Kwong (CORK) equation of state of Holland & Powell (1991, 1998). The surface permeability  $k_\phi$  is kept at  $10^{-16} \text{ m}^2$ ;  $k_\phi$  decreases with depth exponentially with the characteristic length scale of 2.5 km to the reference background value  $10^{-19} \text{ m}^2$  (Manning & Ingebritsen, 1999). The porosity–permeability relationship is the one proposed by Walder & Nur (1984):

$$k_\phi = k_{\phi 0} \left( \frac{\phi^n - \phi_{\min}^n}{\phi_0^n - \phi_{\min}^n} \right)$$

The reference value for porosity is 0.05%. The model is solved using the finite difference method; the grid size is 2.0 km in horizontal dimension and 0.5 km in vertical dimension; the time step is 0.01 Myr.

The model  $P$ – $T$ – $t$  paths in Figs 2–8 are computed for a crustal column located at  $x = 20$  km; model time points are plotted every 0.5 Myr for models with erosion rate 1 m year<sup>-1</sup>, and every 1 Myr for erosion rate 0.5 mm year<sup>-1</sup>. Pressures are calculated using a density of 2800 kg m<sup>-3</sup>; temperature values for points between the grid nodes are computed by linear interpolation.

### Metamorphic reactions in metacarbonate rocks

The heats of metamorphic reactions in metacarbonate rocks are estimated based on the field data for the Waits River Formation in eastern Vermont (Ferry, 1992). The method for these calculations was proposed by Ferry (1983) in his study of metacarbonate-bearing rock sequences in Maine.

The heat absorbed or liberated by reaction,  $Q_r$ , is given by:

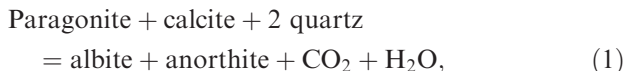
$$Q_r = \sum_l \xi_l \Delta H_l,$$

where  $\xi_l$  is the reaction progress variable for reaction  $l$ ,  $\Delta H_l$  is the enthalpy change for reaction  $l$ , and the sum is over all reactions  $l$  occurring in the rock (e.g. Ferry, 1983).  $\xi_l$  is obtained from:

$$\xi_l = \frac{m_{s,l}}{n_{s,l}},$$

in which  $m_{s,l}$  is the number of moles per volume of phase  $s$  consumed (negative) or produced (positive) by  $l$ , and  $n_{s,l}$  is the stoichiometric coefficient of  $s$  in the reaction (positive for products, negative for reactants). In the following discussion it is assumed that rock volume changes were negligible.

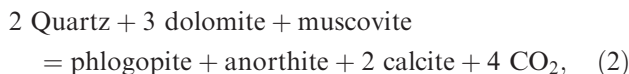
A model reaction for the transition from the ankerite–albite zone to the ankerite–oligoclase zone of the Waits River Formation in Vermont is:



where anorthite and albite are components of plagioclase. Following Ferry (1983), it is assumed that the enthalpy change for model reactions adequately represents that for the actual reactions. Because the heats of prograde Fe–Mg exchange, Na–K exchange and other solid solution effects are not considered, the enthalpy changes based on pure solids probably underestimate those of the actual reactions to some degree. Reaction enthalpies were calculated at 0.8 GPa using the equilibrium temperatures given by Ferry (1992) and the thermodynamic data set of Berman (1988, 1991).

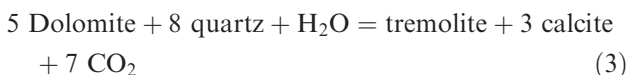
According to the reactions in table 6 in Ferry (1992), the average amount of paragonite consumed was  $-0.0594 \text{ mol l}^{-1}$ , so  $\xi_1 = 0.0594$ . Given that  $\Delta H_1 = 148.3 \text{ kJ mol}^{-1}$ , the average  $Q_r$  was  $8.8 \text{ kJ l}^{-1}$ .

The transition to the biotite zone is modelled according to:



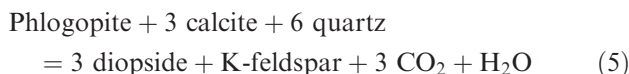
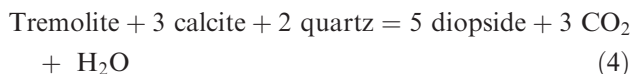
in which anorthite is a component in plagioclase. The average amount of biotite produced (equal to the reaction progress) was  $0.474 \text{ mol l}^{-1}$ , and  $\Delta H_2 = 334 \text{ kJ mol}^{-1}$ . Consequently, the average  $Q_r$  was  $158.3 \text{ kJ l}^{-1}$ .

The model reaction for the transition to the amphibole zone was taken as:

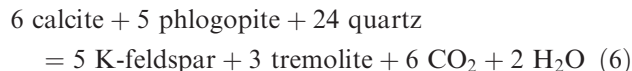


The average amount of amphibole produced was  $0.173 \text{ mol l}^{-1}$ , and  $\Delta H_3 = 460.9 \text{ kJ mol}^{-1}$ . Thus, the average  $Q_r$  was  $79.7 \text{ kJ l}^{-1}$ .

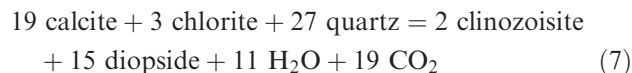
The two primary model reactions for the transition to the diopside zone are:



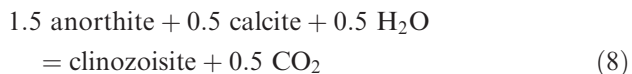
In addition, for some rocks, the production of amphibole can be modelled by another common reaction:



Furthermore, some rocks contained chlorite which broke down during diopside formation, probably according to a reaction similar to:



Finally, clinozoisite was produced by the well-known reaction:



in which anorthite is a component in plagioclase.

An average of  $-0.0606 \text{ mol l}^{-1}$  amphibole was consumed during diopside production, so  $\xi_4 = -0.0606/-1 = 0.0606$ . The average amount of chlorite consumed was  $-0.0505 \text{ mol l}^{-1}$ . Thus,  $\xi_7 = -0.0505/-3 = 0.0168$ . The remaining diopside was modelled to have been produced via reaction 5. Then  $\xi_5 = (m_{\text{Di,tot}} - 5\xi_4 - 15\xi_7)/3 = 0.808 \text{ mol l}^{-1}$ . Here,  $m_{\text{Di,tot}}$  is the average total amount of diopside in the rocks ( $2.979 \text{ mol l}^{-1}$ ). Based on the average amount of amphibole produced,  $\xi_6 = 0.0256/3 = 8.533 \times 10^{-3} \text{ mol l}^{-1}$ . Finally, clinozoisite is inferred to have been produced by both reactions 7 and 8. Thus  $\xi_8 = m_{\text{Czo,tot}} - 2\xi_7 = 0.3788 \text{ mol l}^{-1}$  ( $m_{\text{Czo,tot}} = 0.4124 \text{ mol l}^{-1}$ ).

The  $Q_r$  for the diopside zone is thus modelled as:

$$\begin{aligned} Q_r &= \xi_4 \Delta H_4 + \xi_5 \Delta H_5 + \xi_6 \Delta H_r + \xi_7 \Delta H_7 + \xi_8 \Delta H_8 \\ &= 0.0606(249.6) + 0.808(236.5) + 8.533 \times 10^{-3} \\ &\quad (428.6) + 0.0168(1669.1) + 0.3788(-35.45), \end{aligned}$$

where the enthalpy changes are in  $\text{kJ mol}^{-1}$ . The estimated  $Q_r$  is therefore  $224.5 \text{ kJ l}^{-1}$ .

Adding the ankerite–oligoclase, biotite, amphibole and diopside zone results together yields the total heat consumed by a litre of rock during prograde heating:  $471.3 \text{ kJ l}^{-1}$ .

Received 16 April 2009; revision accepted 6 August 2009.